# CHAPTER II
# LITERATURE REVIEW

## 2.1 Surfactant

A surfactant, or surface active agent, is a chemical substance that is the most versatile product in the chemical industry. Surfactants are used in automobiles, detergents, pharmaceuticals, and are also applied to many high technology areas.

### 2.1.1 Fundamentals of surfactants

A Surfactant, surface active agent, consists of two different structural groups, as shown in Figure 2.1. One is the hydrophilic head group and the other is hydrophobic tail group.

In general, the molecules at the surface or interface have higher potential energy than these in the interior because the interaction between same substances is stronger than that between different substances. When the surfactant is dissolved in a solvent, the lypophobic group of the surfactant in the interior of the solvent causes an increase in free energy of the system. Therefore, displacement of the surfactant molecules to the surface or interface is easier than that of the solvent molecule. From these reasons, the amphipathic structure of the surfactant is the cause of

(1) High concentration of surfactant at the surface,

(2) Reduction of the surface tension of water, and

(3) Orientation of the surfactant molecules at the surface or interface in the aqueous phase.

Surfactants are one of the most unique chemical compounds, having the property of adsorbing onto surfaces or interface of the system and of altering to a marked degree the surface free energies of these surfaces. (Srinarang.2004)[14]

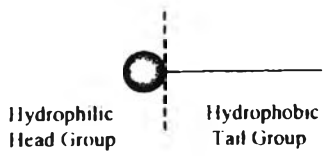


**Figure 2.1** A surfactant molecule (Rosen.1989)[15].

The surfactant can be classified into four categories, which depends on the nature of the hydrophilic group. (Bowornprasirtkul.2002)[16]

1. **Anionic surfactant**: The hydrophilic group consists of a negative charge; for example, $RC_6H_4SO_3^-Na^+$ (alkylbenzene sulfonate).

2. **Cationic surfactant**: The hydrophilic group consists of a positive charge; for example, $RNH_3^+Cl^-$ (salt of long chain alkyl amine).

3. **Zwitterionic surfactant**: The hydrophilic group may give both negative and positive charge; for example, $R^+NH_2CH_2COO^-$ (long-chain amino acid).

4. **Nonionic surfactant**: The hydrophilic group does not contain any ionic charge; for example, $RCOOCH_2CHOHCH_2OH$ (monoglyceride of long-chain fatty acid).

Figure 2.4 illustrates an adsorption isotherm for an ionic surfactant adsorbed on an oppositely charged hydrophilic surface.

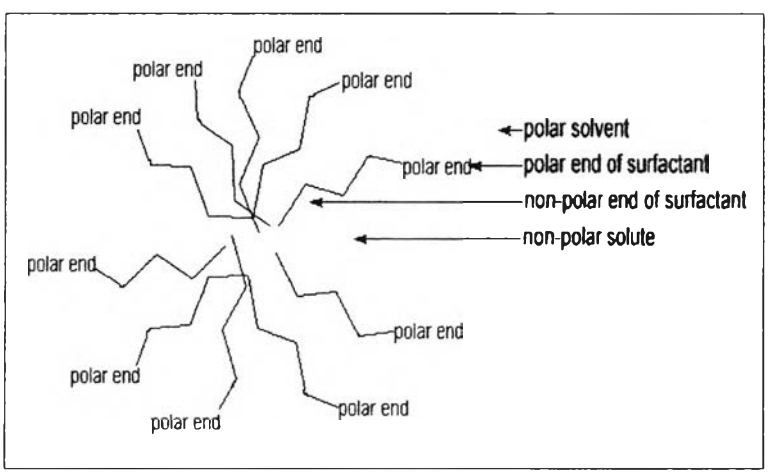


**Figure 2.2** Molecular structure of a surfactant (Chantarak. 2006)[12].

In aqueous solution, surfactant molecules nucleate to form micelles at concentrations higher than the **critical micelle concentration** (CMC). The CMC is a

specific characteristic of each surfactant. Surfactants can form at least three different types of aggregates: Monolayer, called a hemimicelle, or bilayer, called an admicelle at the liquid-solid interface, a micelle in solution, and a monolayer aggregate at the air-liquid interfaces, as shown Figure 2.3.

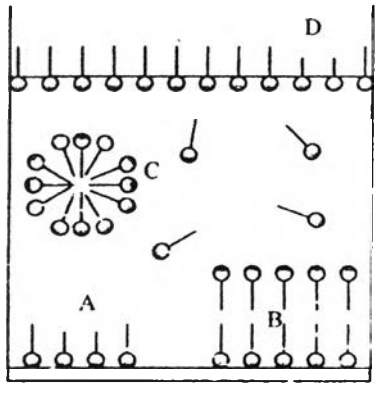


A : Hemimicelle
B : Admicelle
C : Micelle
D : Monolayer aggregate at air-liquid interface.

**Figure 2.3** Surfactant aggregates. (Rosen. 2004)[15].

Surfactant adsorbs onto the solid surface at the interface to form hemimicelle and admincelle aggregate that can be quantified by adsorption isotherm. Surfactant adsorption is one of its singularly important features in an oriented fashion. This property has been studied and applied in many areas, such as detergent to remove soil or dust from clothes and the adsorption polymerization process that has been increasingly utilized in nanocoated film of polymer onto substrates for various purposes.

### 2.1.2 Adsorption of Surfactant at Solid-Liquid Interface

The adsorption of a surfactant at the solid-liquid interface is strongly influenced by three main factors:

1) the grouping of the natural structure, of solid surface whether the surface contains a highly charged site or essentially nonpolar groupings, and the nature of atoms of which these sites or grouping are constituted (e.g. polar group, or nonpolar group);
2) the molecular structure of the surfactant as the adsorbate, whether it is ionic or nonionic and whether the hydrophobic group is long or short,

straight-chain or branched, aliphatic or aromatic. (e.g. anionic, cationic, or nonionic surfactant); and,

3) the surrounding aqueous phase – its pH, its electrolyte content, the presence of any additive, such as short-chain polar solutes, and its temperature (e.g. pH, electrolyte content, and temperature).

These factors can influence the mechanism of adsorption. Generally, there are many types of mechanisms of surfactant adsorption onto substrates involving single ions. These mechanisms consist of ion exchange, ion pairing, acid-base interaction, adsorption by polarization of π electrons, and adsorption by dispersion forces. (Bitting, D. 1985)[17]

In a solid aqueous system, the adsorption isotherm has been studied to understand the behavior of the surfactant on a solid surface and in solution. The amount of surfactant adsorption per unit mass or unit area of solid adsorbent is a convenient way to indicate the amount of adsorbent cover in a constant-temperature system. The amount of adsorbed surfactant can be calculated from the simple basic equation:

$$n_l^s = \frac{\Delta n}{m} = \frac{(\Delta C)V}{m} \qquad (2.1)$$

where

$n_l^s$ = the number of moles of adsorbed surfactant per gram of solid adsorbant at equilibrium,

$\Delta n$ = the change in the number of surfactant molecules in solution,

m = the mass of the adsorbant in grams,

$\Delta C$ = the change of the molar concentration of surfactant in solutions.

V = the volume of liquid phase in liters.

From the number of moles of surfactant adsorbate per gram, $n_l^s$ , the surface concentration, $C_l^s$, in mol/cm$^2$ of surfactant adsorbate can be calculated when the

surface area per unit mass of solid adsorbant ($a_s$) in $cm^2$/ g, or specific surface area, is known. The calculation equation is:

$$C_l^s = \frac{(\Delta C)V}{a_s x m} \tag{2.2}$$

Either $n_l^s$ or $C_l^s$ can be chosen to plot the adsorption isotherm curve. The surface area per adsorbate molecule on substrate, $a_l^s$, in square angstroms, may be calculated from the adsorption isotherm curve by the following equation:

$$a_l^s = 2x\frac{10^{16}}{NC_l^s} \tag{2.3}$$

The $a_l^s$ of the completely formed admicelle can be obtained by using $C_l^s$ from the curve at CMC, and N is avogadro's number.

Many studies have been reported on the adsorption of surfactant on high surface area solids such as metal or glass. Somasundarn and Furerstenau (1996) were the first introduce the adsorption isotherm shape obtained for surfactant on alumina. (Chantarak S. et. al., 2006)[12]

**The shape of an adsorption isotherm curve can be classified into 2 types depend on the adsorbent.**

*2.1.2.1 S-Shaped curve*

The curve has shown an S-shape that can be divided into four regions by following the change in the slope that is related to the phenomena of surfactant adsorption at the solid interface. (Bitting. D. 1985)[17]

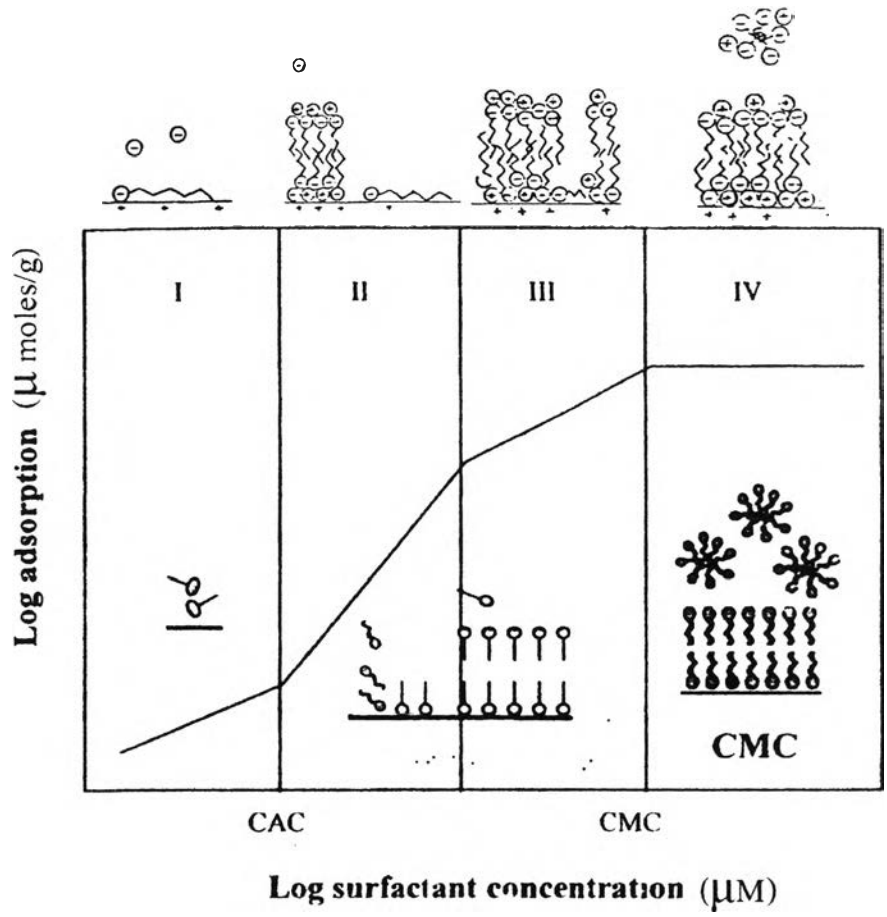


**Figure 2.4** Typical adsorption isotherm of a surfactant in solution (S-shaped curve). (Pongprayoon.et.at..2002)[11].

**Region 1** is commonly referred to as the Henry's law region because there is a unique slope describing the adsorption under low concentration of surfactant. The equilibrium adsorption is proportional to the surfactant concentration in the solution. The drive for the adsorption is largely due to the electrostatic attraction between the charge surfactant species and the oppositely charged mineral oxide surface. As a result of sparsely adsorbed surfactant ion in Region 1, there is little or no interaction between individually adsorbed surfactant ions. It could be generally accepted that the surfactant/ surfactant interactions are negligible in this region. However, there can be significant interaction between the hydrophobic tail and the surface as evidenced by calculations of the chemical potential change per methylene group for monomers adsorbing out of solution.

**Region 2** is characterized by a sharp increase of the slope. This slope of the isotherm indicates a cooperative effect of adsorption with the increase of surface coverage and an enchancement of the affinity of surfactant to the surface.

At this concentration, the surfactants start to aggregate on the substrate and the changing point from Region 1 and 2 is called "**Critical admicellar concentration**" or "**CAC**". (Bitting D.1985)[17]

**Region 3** is characterized by a decrease in slope with the increase of surfactant adsorption. According to Harwell (1985)[18], a common explanation for adsorption behavior in this region is that with increasing adsorption of like-charged head groups on the surface, they begin to repel each other under the action of columbic repulsion force. Another fine distinction may be expressed as the more energetic site offering more favorable adsorption density in Region 2 than the less energetic site in Region 3. Besides the electrostatic effect, there is always the hydrophobic interaction effect present in the tail-tail interactions of the surfactant in both regions.

In the final region, **Region 4**, the adsorption level is nearly constant while total surfactant concentration increase. In this region, the surface concentration of adsorbed surfactant has reached a saturation point, so a further addition of surfactant is only distributed to the bulk liquid. This plateau adsorption is due to the formation of micelles to account for the excess amount of surfactant added to the system. The concentration at which micelle formation begins, or the changing point from Region 3 to 4, is called the "**Critical Micelle Concentration**" or "**CMC**". Surfantant surface coverage can be limited either by the attainment of CMC below bilayer coverage at low surface charge densities or by the attainment of bilayer coverage below CMC at high surface charge densition (Scamehorn et al.,1982)[19]. In either case, the adsorbed surfactant adsorption remains constant with further increase in surfactant concentration.

**Parameters for surfactant adsorption**

The important parameters for surfactant adsorption are the structure of the substrate surface, the molecular structure of the surfactant, and the environment of the aqueous phase.

The most critical parameter is pH of the solution, relative to the pH at which the surface exhibits a net surface charge of zero (or point of zero charge, PZC) as shown in Figure 2.5.

At pH values below the PZC, the surface becomes protonated and more positively charged. At pH values above the PZC, the surface is negatively charged. Therefore, anionic surfactants adsorb well below PZC and cationic surfactants adsorb above PZC.

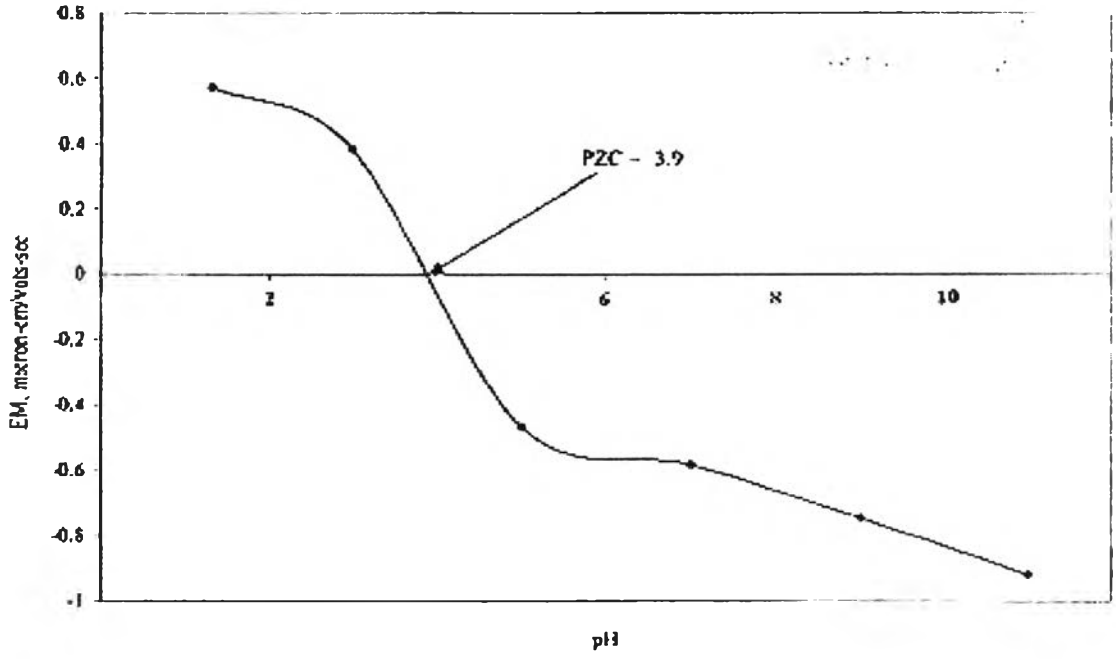


**Figure 2.5** Point of zero charge on a natural rubber surface (Bunsomsit. K. 2002)[10].

Wu et al..(1988)[20] studied the adsorption of an anionic surfactant, **sodium dodecyl sulfate, SDS**, on the solid surface of alumina. The PZC of the alumina was pH 9.5 at 30°C, thus the solution was adjusted to pH 4.0 to be suitable for the anionic surfactant.

*2.1.2.2 L-Shape curve*

The adsorption isotherm of a surfactant from aqueous solution onto nonpolar, hydrophobic adsorbents gives an adsorption isotherm curve in the form of Langmuir type or L-shape curve as shown in Figure 2.6.

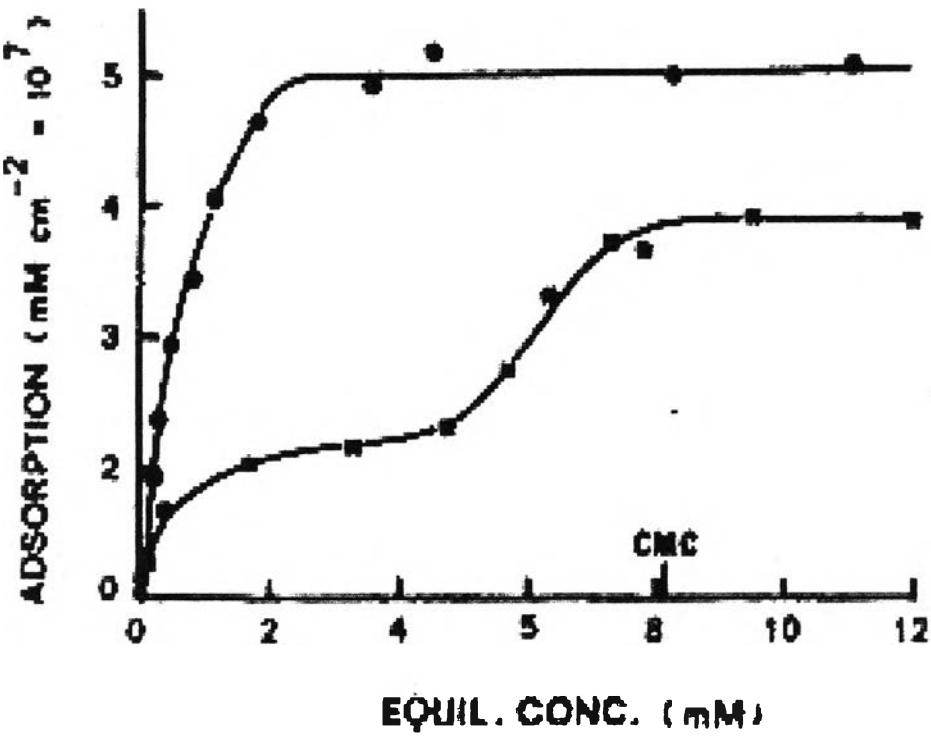


**Figure 2.6** Adsorption isotherm of a surfactant from aqueous solution onto nonpolar, hydrophobic adsorbents.(L-shaped curve) (Rosen ,1989).

The hydrophobic tails of the surfactant are adsorbed on the solid surface, so the orientation of the molecules of surfactant is mostly parallel to the surface. When the molecules of surfactant continue to adsorb on the surface, the orientation is more and more perpendicular to the surface. The inflection point may be from the change of orientation from parallel to perpendicular (Rosen. M.J. 1989).[15]

## 2.2 Admicellar Polymerization Technique

An admicellar polymerization technique is based on the physically adsorbed surfactants onto the substate, so called admicelle. The feasibility of the phenomena of admicelle formation and adsolubilization to form polymerized and organized ultrathin film of molecular dimension on substrates has been investigated for several years (Dunn,1997)[17]. Wu et al. (1993)[20] were the first to propose the formation of styrene-sodium dedecyl sulfate (SDS) on alumina by this polymerization. The bilayer structure of this polymerization is shown in Figure 2.7.

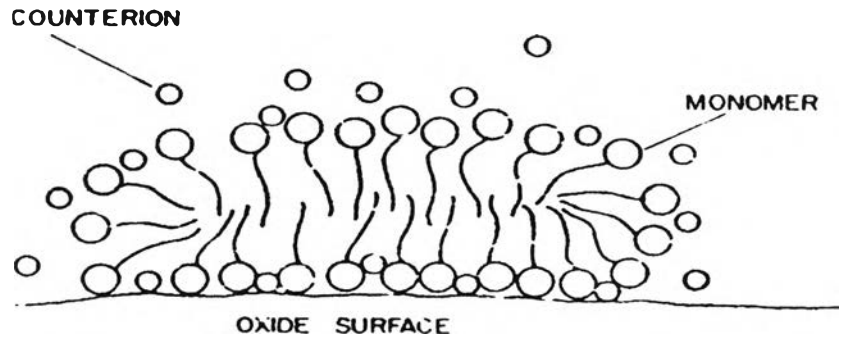


**Figure 2.7** Formation of a sodium dodecyl sulfate admicelle on an alumina surface (Bunsomsit.2002)[10].

Thin flim coating by admicellar polymerization can be divided into four steps as shown in Figure 2.8 (a-d).

### 2.2.1 Step 1: Admicelle Formation

The formation of an admicelle (Harwell et al..1985)[18] occurrs by the adsorption of a surfactant bilayer at the solid/ aqueous solution interface(Figure 2.8 a). The surfactant aggregate formation at the surfactant concentration below the critical micelle concentration (CMC) is manipulated by the solution pH, counterion concentration, and surfactant structure (Scamehorn et al..1982)[19]. The common parameter used to manipulate the admicelle formation is the solution pH at which the substrate surface exhibits a net zero charge (the point of zero charge, PZC).

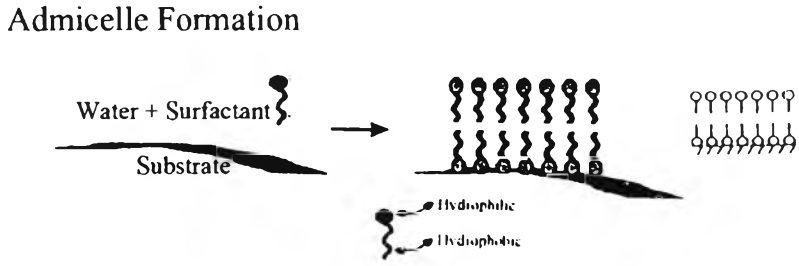


**Figure 2.8a** Admicelle formation of polymerization process (Wongpun T. 2004).[21]

2.2.2 Step 2: Monomer Adsolubilization

The partitioning of organic solutes from aqueous solution into the interior of adsorbed surfactant aggregates is termed adsolubilization. The suggested definition of adsolubilization is "the incorporation of a compound into surfactant surface aggregates, which compound would not be in excess at the interface without surfactant". This phenomenon is an analogue of solubilization, with the adsorbed surfactant bilayer playing the role of micelles, as shown in Figure 2.8b-1, and Figure 2.8b-2.

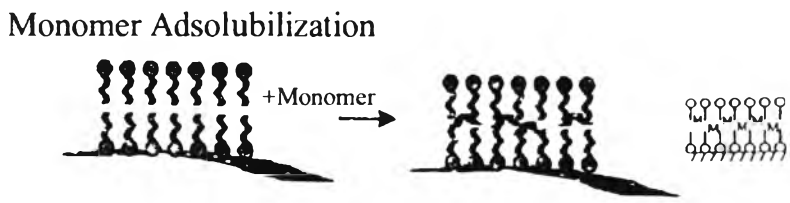


**Figure 2.8b-1** Admicelle Adsolubilization of polymerization process (Wongpun T. 2004).[21]

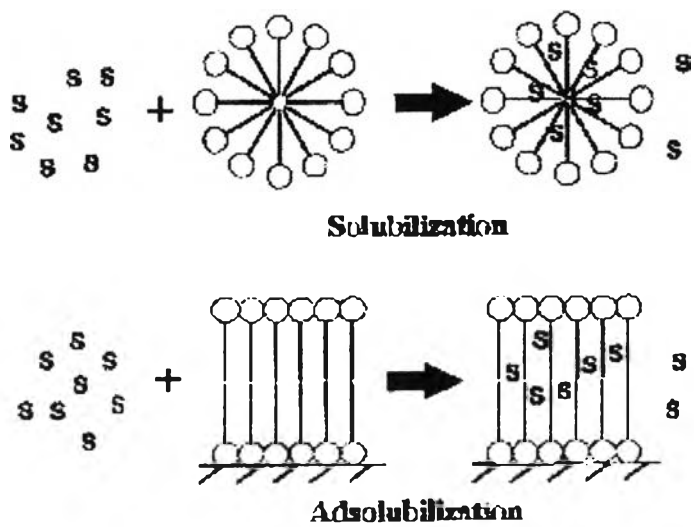


**Figure 2.8b-2** Solubilization and adsolubilization phenomena (Chantarak. S.2006).[12]

2.2.3 Step 3: Polymerization of adsolubilized monomer

The monomer concentrated at the surfactant bilayers (step2) is reacted with a water-soluble initiator. The polymerization is occurred and the monomers are converted to polymer (Figure 2.8 c).

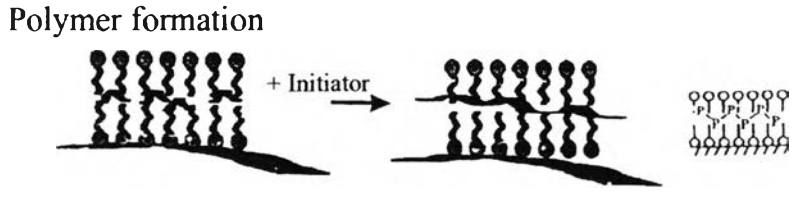


**Figure 2.8c** Polymer formation of polymerization process (Wongpun T. 2004).[21]

2.2.4 Step 4: Surfactant removal

After the polymerization is complete, the upper layer of the surfactant (excess surfactant) is removed by washing. In order to obtain an ultrathin polymer film, the excess surfactant is removed by washing with water (Figure 2.8 d)..

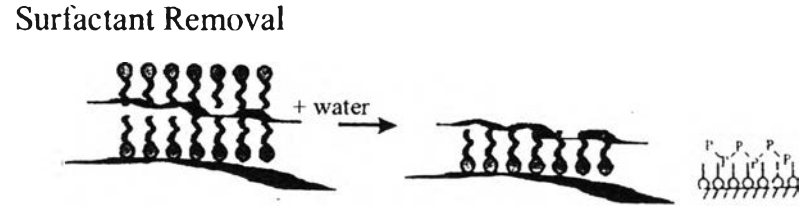


**Figure 2.8d** Surfactant removal of polymerization process (Wongpun T. 2004)[21].

This technique is simple with low energy consumption and is more economical than other coating techniques.

## 2.3 Natural Rubber [2],[22],[23]

Although natural rubber can be isolated from more than a thousand different species of plants, the Para rubber tree, *Hevea brasiliensis*, is practically the sole source of comercial rubber today. The tree is indigenous to the Amazon valley. Natural rubber has been known to the inhabitants of South America for centuries. Christopher Columbus is considered to be the first European to discover it during his second voyage in 1493-1496. Rubber was introduced to the western world by **Chareles**

**de la Condamine**, who sent samples to France from Peru in 1736 and published the result of his observations in 1745. By the end of the eighteenth century, Europe and America were using a few tons of rubber per year. However, users found it difficult to work with solid rubber. Moreover, articles made from natural rubber turned sticky in hot weather and stiffened in the cold.

Two important developments in the nineteenth century enabled these problems to be solved and laid the foundation for the multibillion-dollar modern rubber industry. In 1820, **Thomas Hancock** invented a machine called the "masticator" that allowed solid rubber to be softened, mixed, and shaped. In 1839, **Charles Goodyear** discovered the process of vulcanization. He found that heating a mixture of rubber and sulfur yielded products that had much better properties than raw rubber.

The British considered the possibility of cultivating rubber in Asia, and the rubber tree arrived in Sri Lanka in 1876 and Malaysia the following year. In 1880, *Hevea seedlings* were widely distributed in Asia. The land used for rubber cultivation and the production of natural rubber has grown steadily, as expected, since World War II. In 1983, more than 7.5 million hectares of land were under rubber cultivation and about 4 million metric tons of rubber were produced. The Southeast Asia region accounted for 80% of the total production, with Thailand the biggest producer, followed by Indonesia and Malaysia. The world production of natural rubber is shown in Table 2.1.

**Table 2.1 World production of natural rubber (2004)**

| Country | Percentage |
|---|---|
| Thailand | 36.33 |
| Indonesia | 21.49 |
| Malaysia | 11.99 |
| India | 8.32 |
| Philiphines | 1.06 |
| Others | 20.81 |
| **Total** | 100 % (8.34 Mil tons) |

Source : XIRSG, Rubber Statistical Bulletin, 2004

### 2.3.1 Natural rubber in Thailand [24],[25]

The data from the Industrial Economics and Planning Division, Ministry of Industry, showed that in 1992 Thailand produced 1,520,000 tons of natural rubber and exported 1,400,000 tons or 92.1% of total production. The remaining 7.9% was used in the country. Since 1994, Thailand has been the biggest in the world production of natural rubber. An area of about 12 million hectares is employed in Thailand for rubber cultivation. In 2004 Thailand produced 302.99 million tons of natural rubber. It is uneconomical to transport preserved field latex over long distances to consumer countries; the normal procedure is to change the latex form before shipment. Therefore, after the natural rubber latex has been collected from the field, it is changed into many forms, which are shown in Table 2.2

**Table 2.2 Different types of rubber in Thailand, 2004**

| Type of rubber | % wt |
|---|---|
| Smoked sheet | 66 |
| Block rubber | 18.3 |
| Crepe rubber | 0.73 |
| Concentrated latex | 9.48 |
| Other rubber | 5.46 |

**Source :** Southern Industrial Economics Center in Thailand

Natural rubber latex is 60% dry rubber content by the concentration method. In 2004, Thailand exported 131,888 tons to the USA, Taiwan, Germany and Singapore and the remaining 32,736 tons was used in the country.

### 2.3.2 Properties of Raw Natural Rubber [24],[25]

Natural rubber latex produced by the *tree Hevea brasiliensis,* consists of particles of rubber hydrocarbon and non-rubber constituents suspended in an aqueous serum phase. The average dry rubber content of latex may range between 30% and 45%. The typical composition of fresh latex is shown in Table 2.3.

**Table 2.3 Composition of fresh latex and dry rubbers**

| Composition | Latex (%) | Dry rubber (%) |
|---|---|---|
| Rubber hydrocarbons | 36.0 | 93.7 |
| Protein | 1.40 | 2.20 |
| Carbohydrates | 1.60 | 0.40 |
| Neatral lipid | 1.00 | 2.40 |
| Glycolipids and Phospholipids | 0.60 | 1.0 |
| Inorganic constituents | 0.5 | 0.2 |
| Others | 0.4 | 0.1 |
| Water | 58.5 | - |

2.3.3 Production of Natural Rubber Latex Concentrate [24],[25]

In general, natural rubber is known as natural rubber (NR) latex. The latex appears in the bark outside the cambium layer in ducts spiraling from the left to right as the latex ascends the tree. These ducts are found in concentric rings around the cambium and are really more concentrated near the cambium.

The procedure to obtain the latex, called tapping, is to make a spiral cut that is made downwards from left to right through the bark of the tree. This cut is manipulated to promote the latex to flow into a receptacle such as a plastic, glass, or earthenware cup. Fresh latex coagulates rapidly after tapping, especially in the ambient temperature. Fresh latex has a pH of 7.0. Bacteria decomposes the sugar substances of latex, and therefore the stability of the latex decreases continually as the pH decreases. Bacteria comes from various places such as the atmosphere, the bark, and from the tapping. The preservation of NR latex was first introduced by Johnson and Norris (1853). They suggested using ammonia as an anticoagulant to the latex. The ammonia acts as an alkali to increase the pH of the fresh latex; thus the bacteria remains inactive and the stability of the latex improves. In addition, the electrophoretic mobility of rubber tends to be negatively charged in a base environment. Fresh NR latex exuded from the tree has a dry rubber content of 33% wt. In industry, the latex is concentrated to about 60% wt, which is economical and uniform in quality.

There are several processes to concentrate latex: (1) evaporation, (2) creaming, (3) centrifuging and electrodecantation.

The freshly-tapped NR latex is a whitish fluid with a density of between 0.975 and 0.980 $g.m^{-1}$, and a pH from 6.5 to 7.0. Its viscosity is variable.

The composition of latex is given below:

| | |
|---|---|
| total solids content | 36% |
| dry rubber content | 33% |
| proteinous substances | 1-1.5% |
| resinous substances | 1-2.5% |
| ash | up to 1% |
| sugars | 1% |
| water | ad. 100% |

Hauser (1962) found that rubber particles were quite pear-shape rather than spherical, and consisted of a tough, hard, elastic shell which enclosed a viscous liquid. However, many studies have reported that the rubber particles are spherical in shape, especially the latex from young trees. It is also suggested that the shape of the latex depends on the age and type of tree.

The structure of the *Hevea brasiliensis* latex is:

| | |
|---|---|
| rubber hydrocarbons | 86% |
| water (dispersed in the rubber hydrocarbons) | 10% |
| proteinous substances | 1% |
| lipid substances | 3% |

Trace metals such as magnesium, potassium, and copper are included with the rubber particles at about 0.05%.

Figure 2.9 shows the structure of the NR latex particles. The NR consists of the protein structure at the outer layer of the surface. The adsorbed layer of protein determines the charge on the particle, electrophoretic mobility, and coacervation characteristics. The lipids associated with rubber particles are sterols and sterol esters, and fats and waxes such as eicosyl alcohol and phospholipids. They are found in the bulk of latex particles. They may be dissolved in rubber hydrocarbons. The phos-

pholipids are adsorbed on the particle and are associated with the protein which are anchored to the rubber.

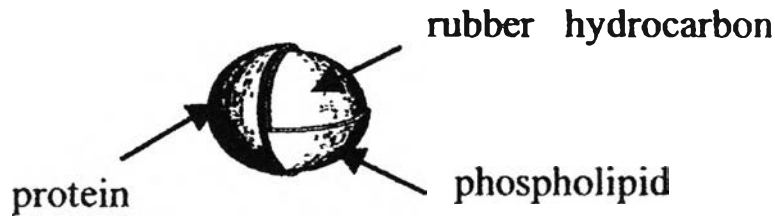


**Figure 2.9** Structure of the NR latex particles (Bunsomsit.2002.)[10].

2.3.4 Chemical formula of natural rubber [2],[26], [27], [28]

The empirical formula for the natural rubber molecule appears to have been first determined by Faraday, who reported his finding in 1826 (Ronald B. 1999)[28]. He concluded that carbon and hydrogen were the only elements present and his results correspond to the formula $C_5H_8$. While this result was obtained using a product which contained associated non-rubbery materials, subsequent studies with highly purified materials have confirmed Faraday's conclusion.

The first, isoprene, was found to have the formula $C_5H_8$ for which Tilden and Dunbrook (1996)[131], proposed the structure shown in Figure 2.10.

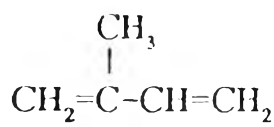

**Figure 2.10** Schematic representation of the structure of a NR latex particle (Bunsomsit.2002).[10]

The linear structure proposed by Pickles[132] provided for the possibility of structure isomerism with both *cis*- and *trans*- repeating units as shown in Figure 2.11.

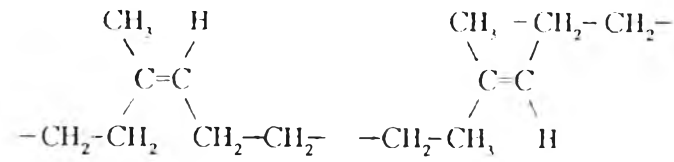

*Cis-* *Tran-*

**Figure 2.11** Schematic representing the structure isomerism with both *cis-* and *trans-* isoprene, repeating units (Bunsomsit.2002.).[10]

It is known that the major hydrocarbon component of both gutta percha and balata (at the time important in belting submarine cable,in golf balls and in container applications) was a polyisoprene which, when reacted with bromine and ozone, gave similar results to those obtained with natural rubber. It was therefore tempting to suggest that one isomer was that of gutta percha and balata and the other of natural rubber. The earlier work of Staudinger suggested that the *trans*-isomer was natural rubber and gutta percha the *cis*-. However, later studies of X-ray fiber diagrams of stretch rubber but Lea Meyer and Mark viewed that natural rubber was the *cis*-polymer, like that observed by Bunn (1942), who elucidated the structure and unit cell (Figure2.12) of the crystalline stretched rubber molecule, as shown in Figure 2.13.

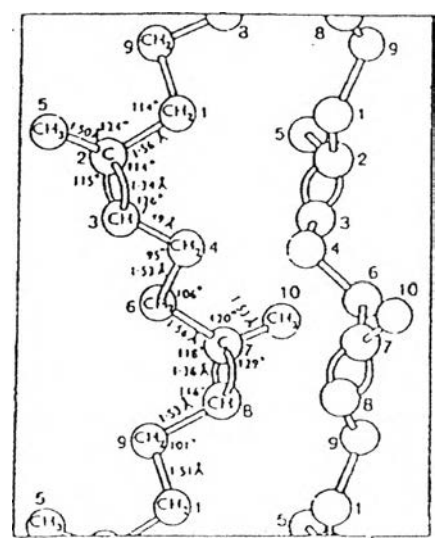

**Figure 2.12** Unit cell structure of the natural rubber molecule. (Brydson J.A..1978)[26].

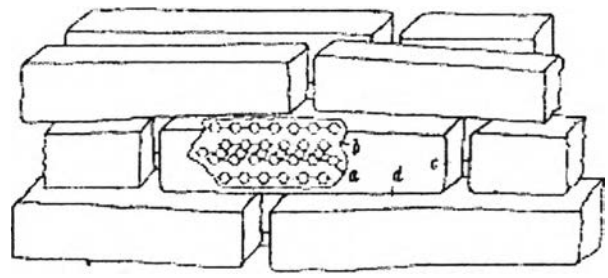


**Figure 2.13** Effects of the stretched rubber molecule (CJB. Clews and F.Schoszberger,1937)[29].

when a = Hauptvalenzketten ; b = intramicellar regions
c = intermicellar holes ; d = intermicellar long spaces

The possibility that the natural rubber molecule might contain a mixture of *cis*- and *trans*- groups was considered to be unlikely because such a mixed polymer would have an irregular structure and be unable to crystallize in the manner of natural rubber. Figure 2.14 illustrates the structure of this rubber, which is *cis*-1,4-polyisoprene.

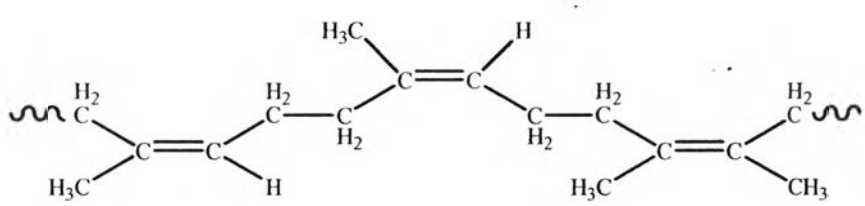

**Figure 2.14** Typical structure of NR latex from *Hevea brasiliensis* (Chantarak, 2006)[12].

Infrared studies have subsequently confirmed that natural rubber was the *cis*-polymer. It has indeed been shown for a long while that natural rubber is at least 97% *cis* 1,4-polyisoprene. The absence of measurable amounts of 1,2- structure but an infrared band at 890 $cm^{-1}$, was at one time thought to be due possibly to the products of a 3,4- structure, as shown in Figure 2.15. (Chantarak, 2006) [12].

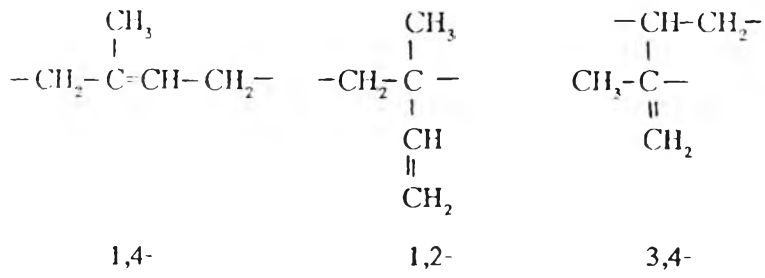


**Figure 2.15** Schematic representation of the structure of *cis*-polymer : *cis*-1,4-polyisoprene (~97%), *cis*-1,2- polyisoprene(~2.7) and *cis*-3,4- polyisoprene(<0.3%) .[2]

Time-averaging techniques using high resolution NMR which are capable of detecting 3,4-groups at a concentration of less than 0.3%, have, however, failed to establish the existence of any such moiety and have also failed to show any trace of *trans*-material. The conclusion must therefore be that the molecule is more than 99% *cis*-1,4-polyisoprene. Since all the evidence points to the conclusion that the natural rubber molecule is not obtained in nature by the polymerization of isoprene, the absence of detectable pendent groups as would be produced by 1,2- and 3,4- addition is hardly surprising.

## 2.4 Electrochemistry

**Electrochemistry** is a branch of chemistry that studies the reactions which take place at the interface of an electronic conductor (the electrode composed of a metal or a semiconductor, including graphite) and an ionic conductor (the electrolyte).

If a chemical reaction is caused by an external voltage, or if a voltage is caused by a chemical reaction, as in a battery, it is an *electrochemical* reaction. In general, electrochemistry deals with situations where an oxidation and a reduction reaction are separated in space. The direct charge transfer from one molecule to another is not a topic of electrochemistry.

Electrochemical synthesis is a common alternative for making conductive polymers (CPs), particularly because this synthetic procedure is relatively straightforward, J. Bargon. (1986) and A.F. Diaz (1979)[30]. Electrochemical preparation of CPs dates back to 1968 when "pyrrole black" was formed as a precipitate on a platinum electrode by exposing an aqueous solution of pyrrole and sulfuric acid to an oxidative potential (A. Dall'Olio 1968)[31].

Today, electrochemical polymerization is performed using a three-electrode configuration (working, counter, and reference electrodes) in a solution of a monomer, an appropriate solvent, and an electrolyte (dopant) (Figure 2.16). Current is passed through the solution and electrodeposition occurs at the positively charged working electrode or anode. Monomers at the working electrode surface undergo oxidation to form radical cations that react with other monomers or radical cations, forming insoluble polymer chains on the electrode surface (Figure 2.17). A number of important variables must be considered, including deposition time and temperature, solvent system (water content), electrolyte, electrode system, and deposition charge. Each of these parameters has an effect on film morphology (thickness and topography), mechanics, and conductivity, which are properties that directly impact the utility of the material for biomedical applications. For example, a non-protic, non-nucleophilic solvent generates stronger and more conductive CPs because protic solvents, like nucleophilic solvents, can generate side reactions with the growing CP chain, limiting and disrupting chain growth.

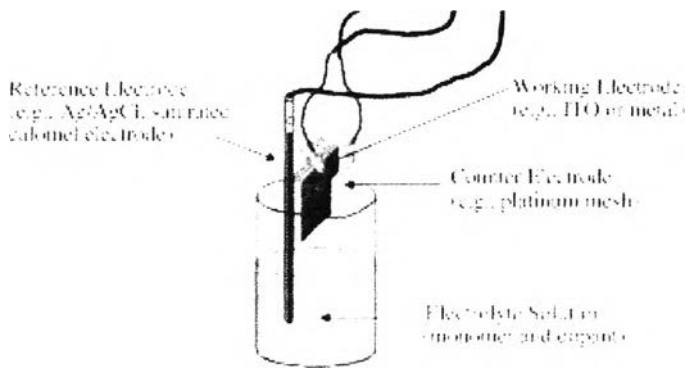

**Figure 2.16** Three electrode setup for electrochemical synthesis: reference electrode, working electrode (where polymerization occurs), and counter electrode all submersed in a monomer and electrolyte solution. (A. Dall'Olio ,1968)[31]

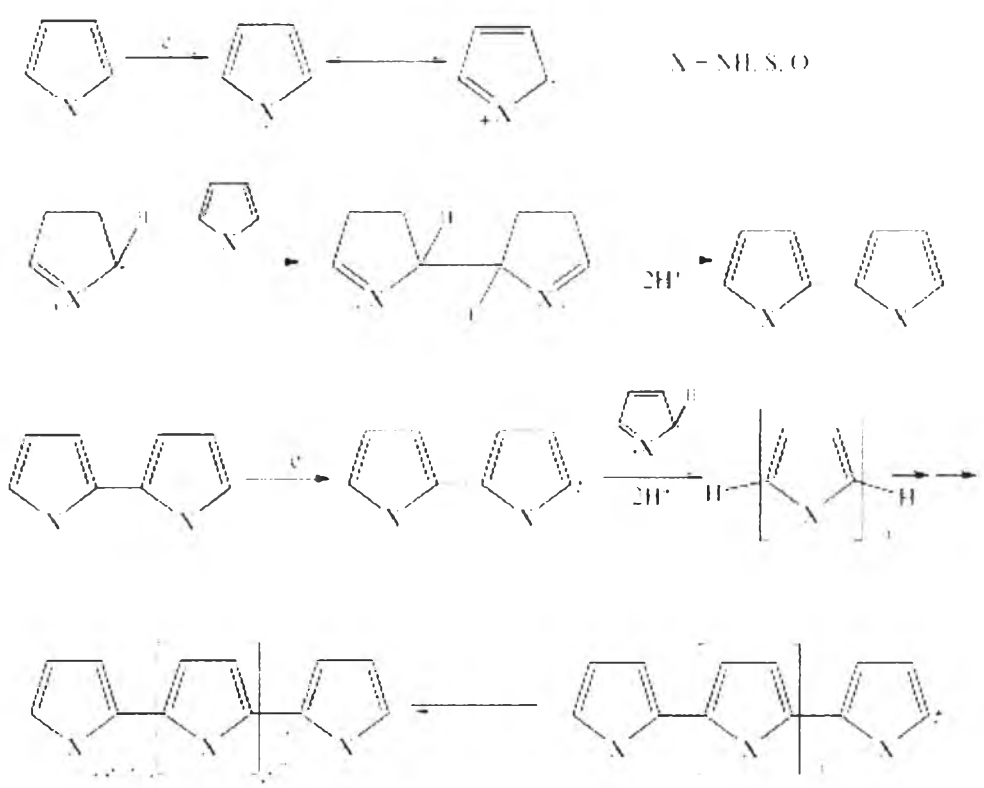

**Figure 2.17** Mechanism for heterocyclic polymerization via electrochemical synthesis. X=NH, S, or O. This pathway is initiated by the oxidation of a monomer at the working electrode to give a cation species, which can react with a neutral monomer species or radical cation oligomeric species to generate the polymer (G. Tourillon., 1986)[32].

The most significant difference between electrochemical and chemical methods of conductive polymer (CP) synthesis is that very thin CP films, on the order of 20 nm, can be produced using the electrochemical technique, whereas powders or very thick films are typically produced with chemical polymerization. All CPs can be synthesized chemically, but electrochemical synthesis is limited to those systems in which the monomer can be oxidized in the presence of a potential to form reactive radical ion intermediates for polymerization. The standard CPs (i.e., PPy, PT, PANI, PEDOT) can be polymerized both chemically and electrochemically; however, several novel CPs with modified monomers are only amenable to chemical polymerization.

### 2.4.1 Cell emf dependency on changes in concentration [32],[33],[34],[35],[36]

#### *2.4.1.1) Nernst Equation*

Calculating a cell's potential is not always plausible at standard temperature and pressure conditions. However, in the 1900s German chemist Walter Hermann Nernst proposed a mathematical model to determine electrochemical cell potential where standard conditions cannot be reached.

In the mid-1800s, Willard Gibbs formulated an equation for a spontaneous process at any conditions,

$$\Delta G = \Delta G^{o} + \mathrm{RT}\ \ln \mathrm{Q} \tag{2.4}$$

where

$\Delta G$ = change in Gibbs free energy,
$T$ = absolute temperature,
$R$ = gas constant,
ln = natural logarithm,
$Q$ = reaction quotient.

Gibbs stated Q's dependency over the reactant and product activity and designated it as their respective chemical activity. Nernst based on Willard Gibbs' work during the mid 19th century, formulated a new equation which replaced $\Delta G$ 's value with the cell's respective maximum electrical work :.

$$nF\Delta E = nF\Delta E^{o} - RT \ln Q \tag{2.5}$$

where

$n$ = number of electrons/mole product,
$F$ = Faraday constant (coulombs/mole), and
$\Delta E$ = electrical potential of the reaction.

Finally he replaced $-nF\Delta E$'s value with electrochemical cell potential, thus formulating a new equation which now bears his name (Nernst equation) :

$$\Delta E = \Delta E^{o} - \frac{\mathrm{RT}}{\mathrm{nF}} \ln Q \qquad (2.6)$$

Assuming standard conditions (Temperature= 298 k, 25°C ) and R = 8.3145 J/Kmol, the equation above can be expressed on Base -10 logarithm as shown below:

$$\Delta E = \Delta E^{o} - \frac{0.0592\ \mathrm{V}}{\mathrm{n}} \log Q \qquad (2.7)$$

### 2.4.1.2) Standard electrode potential

The standard reduction potentials table is determined in a modified version of galvanic cell using hydrogen electrode as cathode. Because hydrogen is taken as reference, the standard reduction potential for that substance is zero (gray highlight) as shown in the Table 2.4.

**Table 2.4 Standard reduction potentials** [32],[33],[34],[35],[36]

**Standard Reduction Potentials at 25°C**

| Reduction Half-Reaction | | E (V) |
|---|---|---|
| $F_2(g) + 2\,e^-$ | $\longrightarrow 2\,F^-(aq)$ | 2.87 |
| $H_2O_2(aq) + 2\,H^+(aq) + 2\,e^-$ | $\longrightarrow 2\,H_2O(l)$ | 1.78 |
| $MnO_4^-(aq) + 8\,H^+(aq) + 5\,e^-$ | $\longrightarrow Mn^{2+}(aq) + 4\,H_2O(l)$ | 1.51 |
| $Cl_2(g) + 2\,e^-$ | $\longrightarrow 2\,Cl^-(aq)$ | 1.36 |
| $Cr_2O_7^{2-}(aq) + 14\,H^+(aq) + 6\,e^-$ | $\longrightarrow 2\,Cr^{3+}(aq) + 7\,H_2O(l)$ | 1.33 |
| $O_2(g) + 4\,H^+(aq) + 4\,e^-$ | $\longrightarrow 2\,H_2O(l)$ | 1.23 |
| $Br_2(l) + 2\,e^-$ | $\longrightarrow 2\,Br^-(aq)$ | 1.09 |
| $Ag^+(aq) + e^-$ | $\longrightarrow Ag(s)$ | 0.80 |
| $Fe^{3+}(aq) + e^-$ | $\longrightarrow Fe^{2+}(aq)$ | 0.77 |
| $O_2(g) + 2\,H^+(aq) + 2\,e^-$ | $\longrightarrow H_2O_2(aq)$ | 0.70 |
| $I_2(s) + 2\,e^-$ | $\longrightarrow 2\,I^-(aq)$ | 0.54 |
| $O_2(g) + 2\,H_2O(l) + 4\,e^-$ | $\longrightarrow 4\,OH^-(aq)$ | 0.40 |
| $Cu^{2+}(aq) + 2\,e^-$ | $\longrightarrow Cu(s)$ | 0.34 |
| $Sn^{4+}(aq) + 2\,e^-$ | $\longrightarrow Sn^{2+}(aq)$ | 0.15 |
| $2\,H^+(aq) + 2\,e^-$ | $\longrightarrow H_2(g)$ | 0 |
| $Pb^{2+}(aq) + 2e^-$ | $\longrightarrow Pb(s)$ | −0.13 |
| $Ni^{2+}(aq) + 2\,e^-$ | $\longrightarrow Ni(s)$ | −0.26 |
| $Cd^{2+}(aq) + 2\,e^-$ | $\longrightarrow Cd(s)$ | −0.40 |
| $Fe^{2+}(aq) + 2\,e^-$ | $\longrightarrow Fe(s)$ | 0.45 |
| $Zn^{2+}(aq) + 2\,e^-$ | $\longrightarrow Zn(s)$ | −0.76 |
| $2\,H_2O(l) + 2\,e^-$ | $\longrightarrow H_2(g) + 2\,OH^-(aq)$ | −0.83 |
| $Al^{3+}(aq) + 3\,e^-$ | $\longrightarrow Al(s)$ | −1.66 |
| $Mg^{2+}(aq) + 2\,e^-$ | $\longrightarrow Mg(s)$ | −2.37 |
| $Na^+(aq) + e^-$ | $\longrightarrow Na(s)$ | −2.71 |
| $Li^+(aq) + e^-$ | $\longrightarrow Li(s)$ | −3.04 |

**Source :** http://en.wikipedia.org/wiki/Image:Reduction-potentials2.PNG

Standard electrode potential is the value of the standard emf of a cell in which molecular hydrogen, under standard pressure ($10^5$ Pa), is oxidized to solvated protons at the left-hand electrode.

The cell potential depends on the difference between each half cell potential. Conventionally, the potential associated with each electrode is chosen as the reduction takes place on the chosen electrode; hence, standard electrode potentials are tabulated on reduction potentials, and thus tables are built on standard reduction potentials noted as $E^0_{red}$.

Standard cell potential is calculated by the difference between the standard reduction potentials of each electrode:

$$E^o_{cell} = E^o_{red}(cathode) - E^o_{red}(anode) \qquad (2.8)$$

The **standard hydrogen electrode, or SHE,** consists of an inverted glass tube similar to a laboratory test tube, where a light and fine platinum wire is connected to a thin platinum blade. This setup is placed in a solution of Hydrochloric acid, plenty of $H^+$ ions, Gaseous hydrogen enters through the tube and reacts over the platinum blade, thus allowing reduction and oxidation processes to occur.

SHE operates exactly the same way as conventional electrodes on Daniells' cell work; in order to measure the standard reduction potential, SHE replaces one of the electrodes in the electrochemical cell acting as cathode or anode, thus electric current generated on the cell represents the standard reduction potential for the element which is measured.

For example on Copper standard reduction potential[31],[32],[33],[34],[35],[36]:

Cell diagram

$$Pt(s)|H_2(1atm)|H^+(1M)||Cu^{2+}(1M)|Cu(s) \tag{2.9}$$

$$E^o_{cell} = E^o_{red}(cathode) - E^o_{red}(anode) \tag{2.8}$$

At standard temperature and pressure conditions, the cell's emf (measured by a multimeter) is 0.34 V (conventionally SHE has a zero value) thus, replacing in the previous equation gives:

$$0.34V_{cell} = E^o_{Cu^{2+}/Cu} - E^o_{H^+/H_2} \tag{2.10}$$

$$0.34V_{cell} = E^o_{Cu^{2+}/Cu} - 0 \tag{2.11}$$

An electrochemical cell's emf value is used to predict whether a redox reaction is a spontaneous process or not. A positive sign for overall cell's standard potential is considered to be spontaneous reaction, a negative sign would predict a spontaneous reaction in the opposite direction.

Changes over the stoichiometric coefficients on the balanced cell equation will not change the $E^0_{red}$ value because standard electrode potential is an intensive property.

2.4.2 Concentration cells

Calculating membrane potential is a good example where concentration cells are used in biology to understanding a cell's metabolism such as in a $Na^+$and $K^+$ pump. A concentration cell is an electrochemical cell whose electrodes are from the same material, differing in ionic concentrations on both half-cells; for example, in an electrochemical cell, where two copper electrodes are submerged on blue vitriol's solution, whose concentrations are 0.05 M and 2.0 M, while connected through wire and a saline bridge.

$$Cu^{2+}(aq) + 2e^{-} \rightarrow \mathrm{Cu}(s) \tag{2.12}$$

**Le Chatelier's principle** indicates that reaction is favorable for reduction as the concentration of $Cu^{2+}$ ions increases. Reduction will take place in a cell's compartment where the concentration is higher, and oxidation will occur on the diluted side.

The following cell diagram describes the cell mentioned above:

$$Cu(s)|Cu^{2+}(0.05M)||Cu^{2+}(2.0M)|Cu(s) \tag{2.13}$$

where both half cell reactions for oxidation and reduction are

$$Oxidation : Cu(s) \rightarrow \mathrm{Cu}^{2+}(0.05M) + 2e^{-} \tag{2.14}$$

$$Reduction : Cu^{2+}(2.0M) + 2e^{-} \rightarrow \mathrm{Cu}(s) \tag{2.15}$$

$$Overall reaction : Cu^{2+}(2.0M) \rightarrow \mathrm{Cu}^{2+}(0.05M) \tag{2.16}$$

where the cell's emf is calculated through the Nernst equation as follows:

$$E = E^{o} - \frac{0.0257\mathrm{V}}{2} ln \frac{[Cu^{2+}]_{diluted}}{[Cu^{2+}]_{concentrated}} \tag{2.17}$$

The $E^{o}$ value of this kind of cell is zero, as electrodes and ions are the same in both half-cells. After replacing values from the case mentioned, it is possible to calculate the cell's potential:

$$E = 0 - \frac{0.0257\mathrm{V}}{2} ln \frac{0.05}{2.0} \tag{2.18}$$

$$E = 0.0474\mathrm{V} \tag{2.19}$$

From the above theories, the electrodes are undergoing a similar reduction reaction but have different concentrations. Due to this difference, there is a difference in potential (voltage) between the electrodes. At the anode, copper atoms dissolve into solution and give up electrons, while at the cathode, copper ions deposit on the electrode and acquire electrons.

## 2.5 The Theoretical consideration of conductive polymer [2],[37],[38],[39],[40]

In order to understand more about conductive polymer, a suitable starting point for consideration is the band theory which is the essential basic of concepts for discussion of conduction in a molecular solid. Since this Research prepared polymer by electrochemical polymerization, the effect of oxidation potential of solution was significant in this study. Furthermore, the measurement of conductivity was described.

### 2.5.1 Band structure [2],[37],[38],[39],[40]

For simplicity, we assume that one atom provides one atomic s-orbital at some energy, Figure 2.18(a). When the second atom is brought up, it overlaps the first one and forms a bonding orbital and an antibonding orbital, Figure 2.18(b). The third is brought up and overlaps its nearest neighbor (and only slightly its next-nearest) and from these, three molecular obitals are formed as shown in Figure 2.18(c). The fourth atom (Figure 2.18(d)) leads to the formation of a fourth molecular orbital, and at this stage we can see that the general effect of bringing up successive atoms is slightly to spread the range of energies covered by the orbital, and also to fill in the range with orbital energies. When N atoms (Figure 2.18(e)) have been slotted on to the line, there are N molecular obitals covering a band of finite width. When N is definitely large, the orbital energies are indefinitely close and form a virtually continuous band. Nevertheless the virtually continuous band consists of N different molecular orbitals; the lowest-energy orbitals in the band bringing predominantly bonding and the highest-energy predominantly antibonding. (Kanatzidis. M.G. 1990)[40].

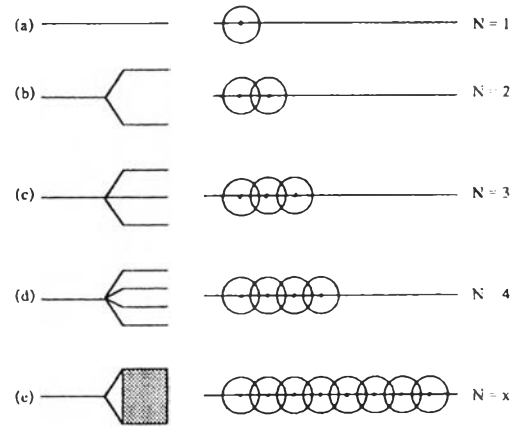


**Figure 2.18** Formation of a band of N orbitals by the successive addition of atoms to a line.

The band formed from S-orbitals is called the s-band. If the atoms carry p-orbitals, the same procedure may be followed, and the band of molecular orbitals is called the p-band, Figure 2.19. If the atomic p-level lies higher than the atomic s-level, the p-band lies higher than the s-band, unless it is so broad (strong overlap) that the bands overlap. (Ruangsiritanyakul, T. 1996)[37]

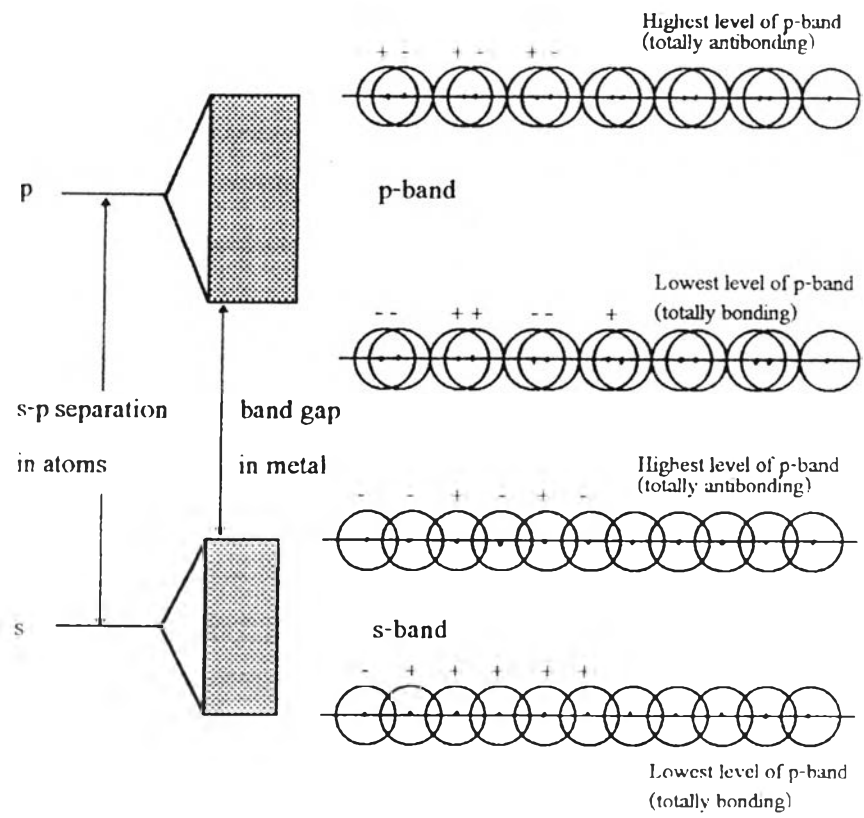


**Figure 2.19** S-band, P-band, and the band gap. (Tasakorn, P. 1996)[2].

### 2.5.2 Metal, Semiconductor, and Insulator [2],[37],[38],[39],[40]

Energy band diagrams may be used to illustrate the difference between metals, semiconductors, and insulators. For a sample model in metals, the electrons completely fill the valence band and partially fill the conductive band. The higher energy conduction band is empty at absolute zero. This is shown in Figure 2.20 (a). Above absolute zero, electrons at the top of the highest occupied level can gain thermal energy and move into the low lying empty levels of the conductive bands. A substantial fraction of the electrons can be excited into singly occupied energy levels, even at relatively low temperature. Such unpaired electrons contribute to the electrical conductivity of a metal, and the substance is called a conductor.

In semiconductors and insulators, shown in Figure 2.20 (b) and (c), the valence band is completely filled and an energy gap exists between it and the next higher energy band. If the energy gap is wide (large), there is little chance for electrons to be excited into an empty conduction band and the material is an intrinsic semiconductor, electrons being excited rather easily into the conduction band. If the gap is wide but impure atoms are added, it may be possible to establish a level within the gap that facilitates the movement of electrons into the conduction band. These latter systems are known as impure semiconductors, or extrinsic semiconductors.

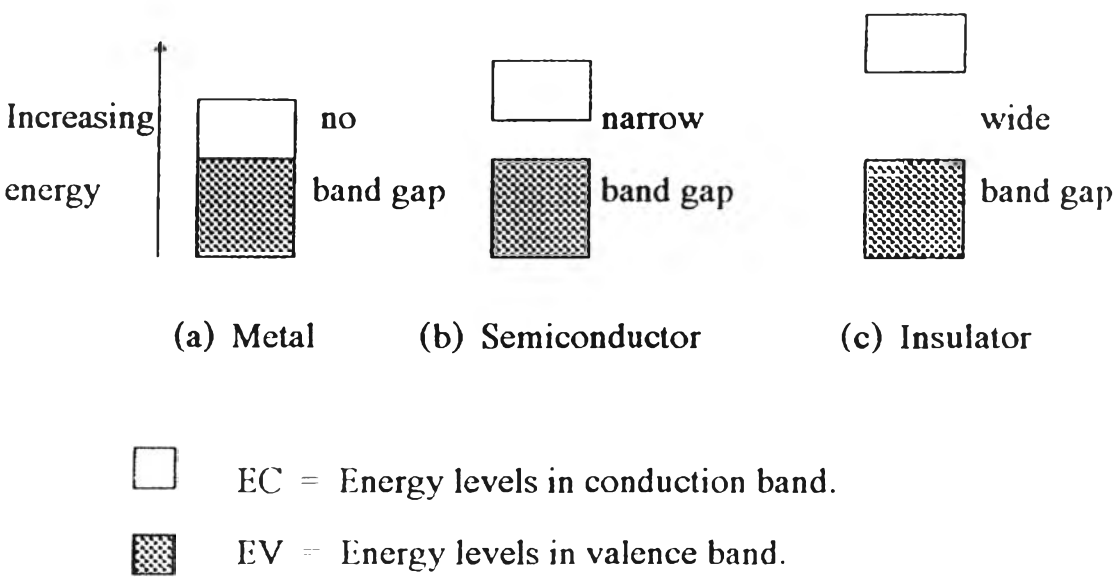


**Figure 2.20** Relationship of energy gaps in the three types of solids.

Conducting polymers are peculiar in that they conduct a current without having a partially empty or partially filled band. Their electrical conductivity cannot be explained well by the simple band theory. For example, the simple band theory cannot explain why the charge carriers, usually electrons or holes, in polypyrrole are spinless. To explain some of the electronic phenomena in these organic polymers, concepts from physics that are new for chemists, including polarons and bipolarons (Figure 2.21), have since the early 1980s been applied to conducting polymers.

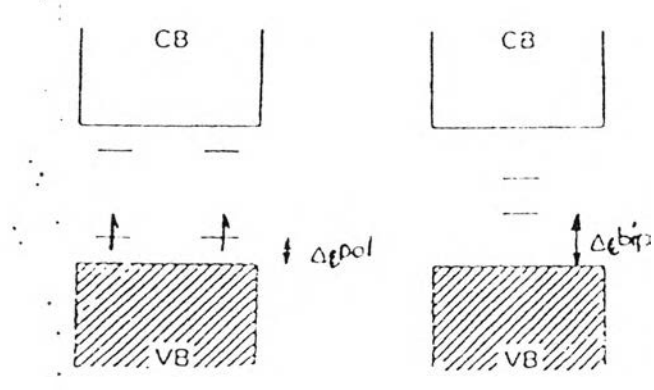


**Figure 2.21** Band structure of a polymer chain containing:

(a) two polarons

(b) one bipolarons

2.5.3 Concept of doping [2].[4].[40].[41]

Conjugated polymers are either electrical insultators or semiconductors, but their resistivity can be decreased by several orders of magnitude by "doping".

Since 1977, polyacetylene $(CH)_x$ has been known as the prototype conducting polymer which can be p- or n-doped, either chemically or electrochemically. The development in the field of conducting polymers has grown rapidly. And a variety of other conducting polymers and their derivatives have been discovered. In the "doped" state, the backbone of a conducting polymer consists of a delocalized $\pi$-system. The doping process can be classified into three processes: redox doping, non-redox doping, and doping involving no dopant ions (Kanatzidis, M.G. 1990)[40].

*2.5.3.1 Redox doping*

The doping of all conducting polymers had previously been accomplished by redox doping. This involves the partial addition (reduction) or removal (oxidation) of electrons to or from the π-system of the polymer backbone.

This can be done by chemical or electrochemical processes during which the number of electrons associated with the polymer backbone changes. Examples of conductive polymers are presented below:

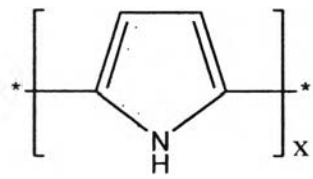


Polypyrrole

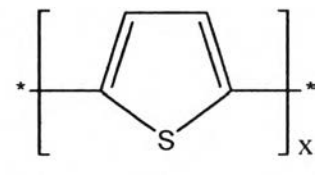


Polythiophene

Doping is the process of oxidizing (p-doping) or reducing (n-doping) a neutral polymer and providing a counter anion or cation (i.e. dopant), respectively. Upon doping, a CP system with a net charge of zero is produced due to the close association of the counter ions with the charged CP backbone. This process introduces charge carriers, in the form of charged polarons (i.e. radical ions) or bipolarons (i.e. dications or dianions), into the polymer (Figure 2.22) (Nathalie K. 2007)[4]. The attraction of electrons in one repeat-unit to the nuclei in neighboring units yields charge mobility along the chains and between chains, often referred to as "electron hopping". The ordered movement of these charge carriers along the conjugated CP backbone produces electrical conductivity. The smaller the band gap (i.e. distance between conducting band and valence band) energy for a CP, the more conductive it is considered to be (Bredas. J.L. 1985)[41].

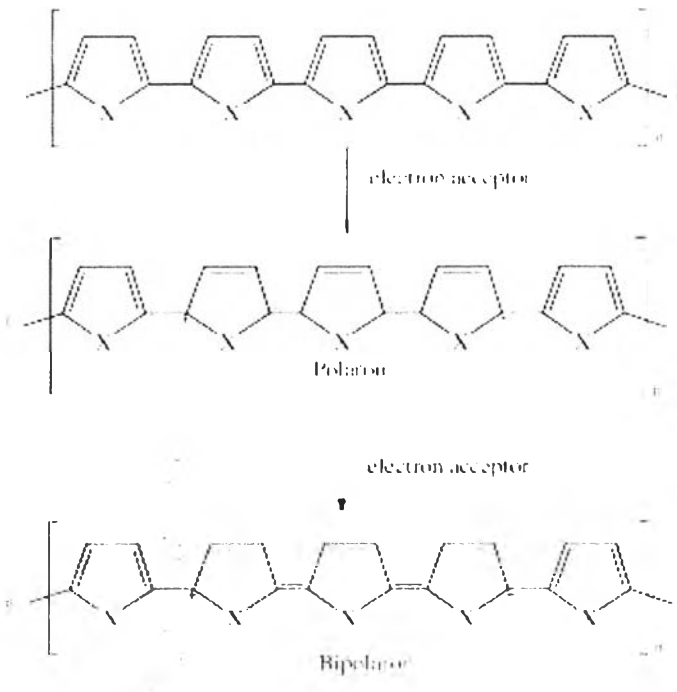

**Figure 2.22** Introduction of polaron and bipolaron lattice deformation upon oxidation (p-type doping) in heterocyclic polymers. X=S, N, or O. A polaron or radical cation is introduced into the conjugated backbone after the loss of an electron. When oxidation of the same segment of the conjugated backbone occurs, the unpaired electron of the polaron is lost and a dication (i.e. bipolaron) is formed.

Figure 2.23 illustrates the change in band structure of PPy and PT subsequent to doping. There are many factors that influence this band gap and thus conductivity, including dopant, oxidation level/doping percentage, and synthesis method and temperature; therefore, there are often discrepancies among the results presented by different research groups—G. Tourillon, (1986)[42], K. Kaneto (1983)[43], T.-C. Chung (1984)[44], and G. Wallace (2004)[45]. The reader is referred to A.J. Heeger (1986, 2002)[46] and J.L. Bredas (1986)[47] for detailed explanations of conductivity mechanisms.

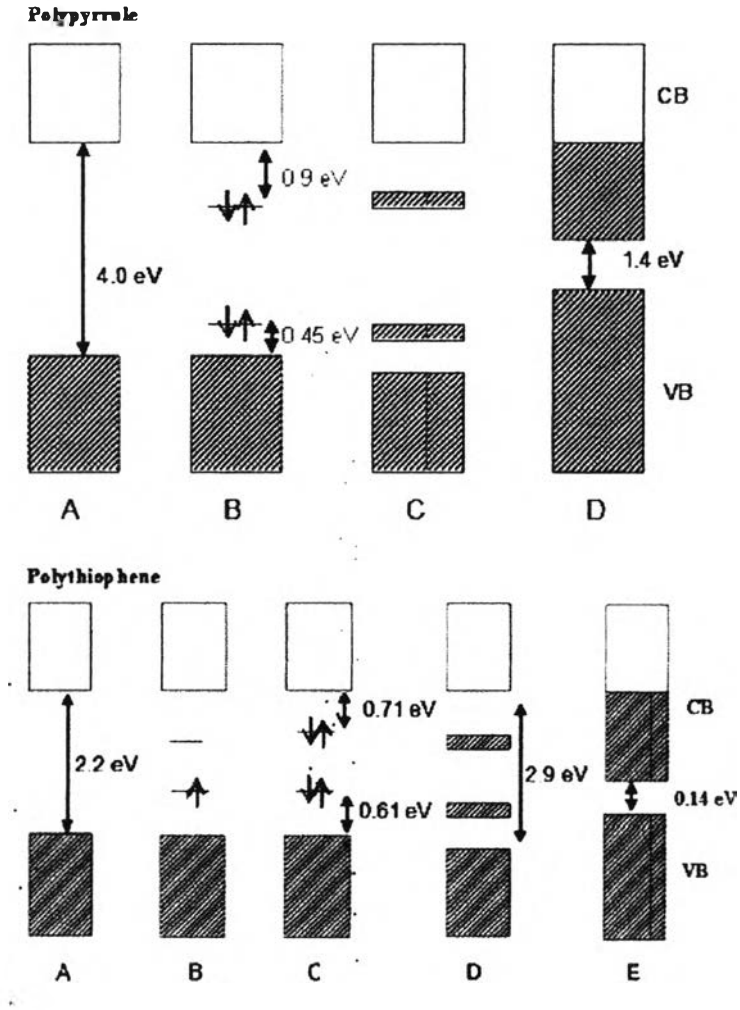


**Figure 2.23** Valence-effective Hamiltonian band structure evolution of PPy (top) and PT (bottom) upon doping.

**PPy (top):**

(A) undoped

(B) intermediate doping level.

Formation of non-interacting bipolarons at 0.45 eV above the valence band (VB) and 0.9 eV below the conductive band (CB).

(C) 33% doping level (experimentally obtained with electrochemical doping). Formation of bipolaron bands with width of 0.25 eV.

(D) 100% doping level per monomer. Merging of bipolaron bands with VB and CB. Note the decrease in band gap from 4 to 1.4 eV.

**J.L. Bredas, (1986)**[47]

**PT (bottom):**

(A) undoped.

(B) 0.1% doping level with polaron states in the gap.

(C) Few ($\sim$1–20%) percent doping level, with the formation of non-interacting bipolarons at 0.61 eV above VB and 0.71 eV below CB.

(D) 30% doping level, where the bipolaron states overlap and form two bands.

(E) Hypothetical 100% doping level, with quasi-metallic behavior. Adapted from G. Tourillon, (1986)[42]

***Doping of polypyrrole*** [2],[4],[21],[40],[45]

In the doping process, counter "dopant" ions are introduced which stabilize the charge on the polymer backbone. The polymer may store charge in two ways.

In an oxidation process it could either lose an electron from one of the bands or it could localize the charge over a small section of the chain. Localization of the charge causes a local distortion due to a change in geometry, which costs the polymer some energy.

In each case, spectroscopic signatures, e.g. those of solitons, polarons, bipolarons, etc. are obtained characterisitic of the given charged polymer. Examples of the polaron and bipolaron structure of a polymer are shown in Figure 2.24.

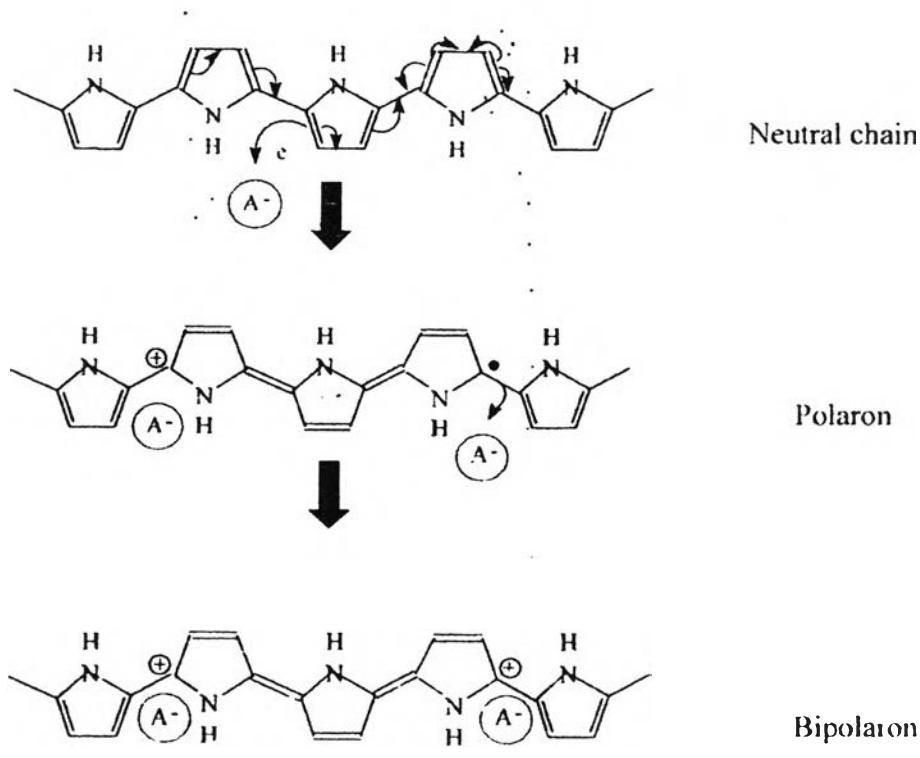


**Figure 2.24** P-type doping of polypyrrole resulting in a polaron and bipolaron.

***Doping of polythiophene*** [21],[45]

In 1986, the electrochemical and chemical synthesis of polythiophene(PTh) was accomplished. Transition-metal halides such as $FeCl_3$, $MoCl_5$ ,and $RuCl_3$ were used for the chemical oxidative polymerization. To enhance the conductivity, it can be doped by many dopants such as iodine, $FeCl_3$, $NOSbF_6$, and $SO_3CF^-$.

PTh can exist in a variety of redox forms, as shown in Figure 2.25. However, the electrical conductivity is assigned usually to only one of them. The withdrawal of one electron from the PTh molecule (Figure2.25(a)), followed by its doping with a solution anion (x-), leads to its half oxidized polaronic state (Figure 2.25(b)), whereas the loss of a second electron leads to the oxidized bipolaronic form (Figure 2.25(c)).

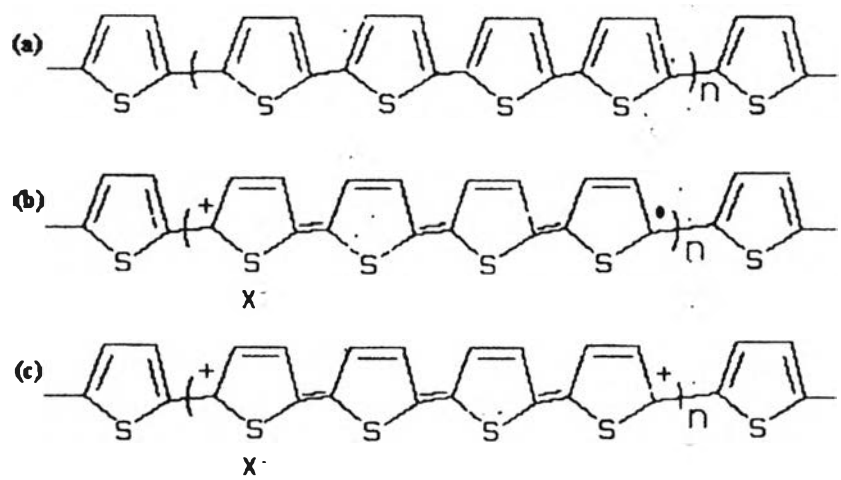


**Figure 2.25** Different redox forms of PTh: (a) reduced; (b) half-oxidized (polaronic) and (c) Oxidized (bipolaronic).

In summary, conduction by polarons and bipolaron is now thought to be the dominate mechanism of charge transport in polymers. These concepts was dependent on the doping of these polymers where its data demonstrate that

(1) Polaron is formed on the chain at low oxidation level (slightly doped polymer)

(2) At high oxidation level, polarons combine to form spinless bipolaron (heavily doped polymer)

(3) Wide bipolaron bands are present in the gap in the highly conductive regime (heavily doped polymer).

## 2.6 Application of organic conducting polymer[48]

The typical conductive polymers, for which most of the work has been done, are summarized in Table 2.5.

**Table 2.5** Typical conducting polymers

| Name | Structure | Name | Structure |
|---|---|---|---|
| *trans*-Polyacetylene | 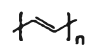 | Poly(phenylene ethynylene) | 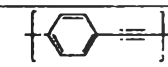 |
| *cis*-Polyacetylene |  | Polyselenophene | 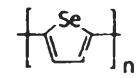 |
| Polypyrrole | 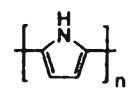 | Polyfuran | 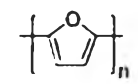 |
| Polythiophene | 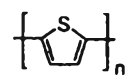 | Poly(*N*-substituted aniline) | 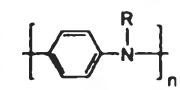 |
| Poly(*p*-phenylene) | 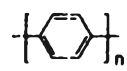 | Poly(*N*-substituted pyrrole) | 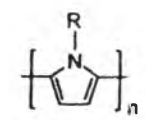 |
| Poly(phenylenevinylene) | 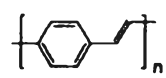 | Poly(diphenylamine) | 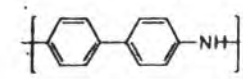 |
| Polyaniline | 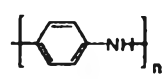 | Poly(indole) | 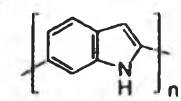 |
| Poly(thienylenevinylene) | 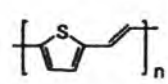 | Poly(thieno[3,2-*b*]pyrrole) | 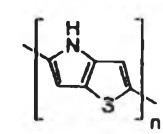 |
| Poly(furylenevinylene) | 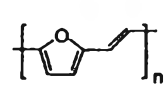 | Poly(fluorene) | 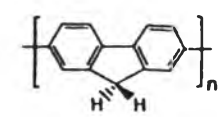 |
| Poly(phenylenesulfide) | 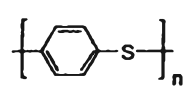 | Polypyridine | 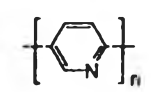 |

Their conductive properties in comparison to those of metals, inorganic, and other organic compounds, are shown in Figure 2.26.

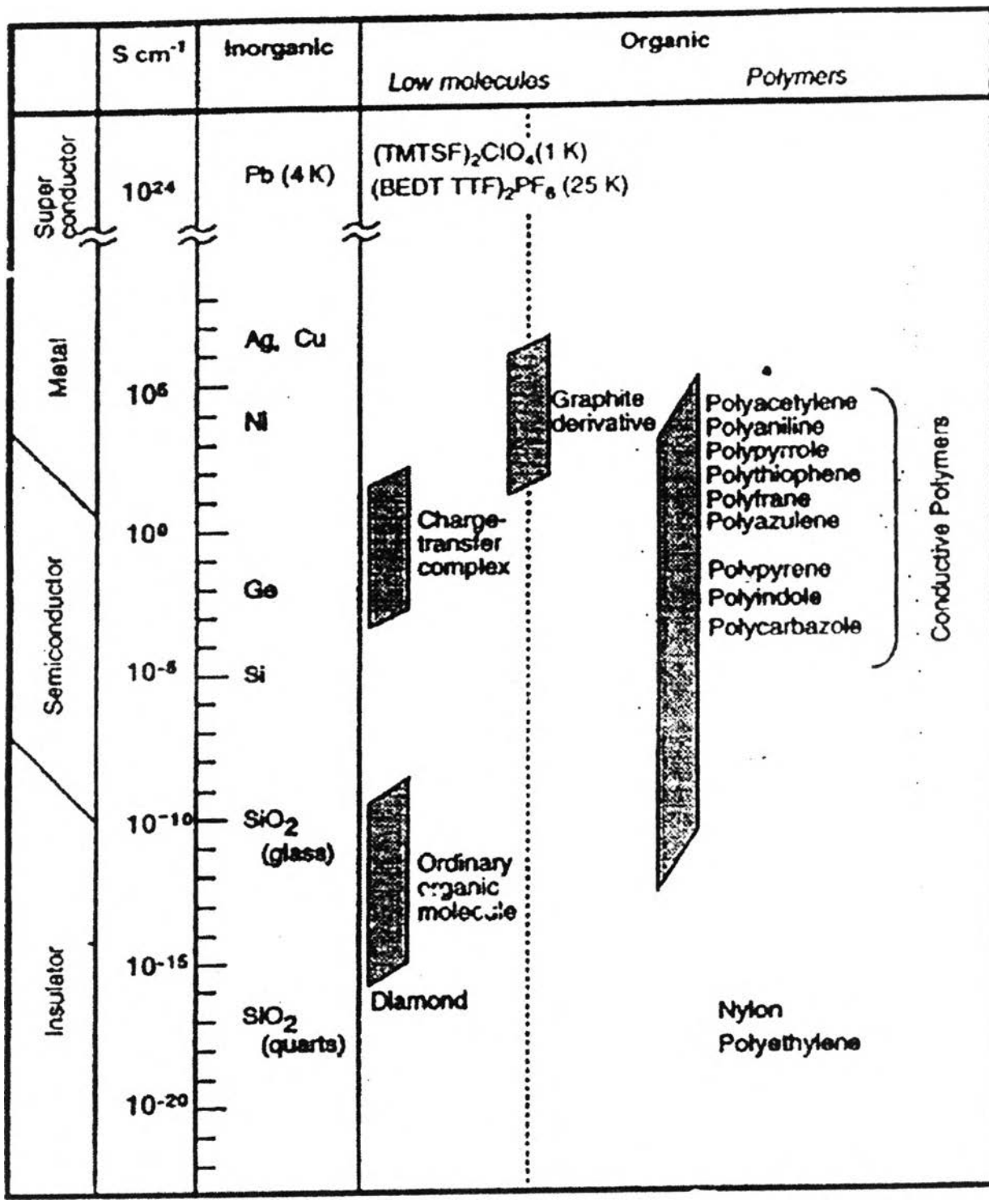


**Figure 2.26** Conductivity of various organic compounds in comparison to inorganic materials (Tepveera, K. et al 2003)[48].

Organic conductive polymers have a unique and practical advantage. Their conductive properties allow the use of electronic tools (computers and interfaces) and other existing and emerging characterization tools to retrieve the information on the behavior of these systems from real *in situ* environments. In addition, their other properties can be manipulated *in situ* using appropriate electronic stimulation (Table 2.6).

**Table 2.6** Change of properties upon electrical stimulation to organic conducting polymers

| **Property** | **Typical Change** | **Potential Application** |
|---|---|---|
| Conductivity | From $10^{-7}$ to $10^{-3}$ $S.cm^{-1}$ | Electronic components sensors |
| Volume | 3% | Electromechanical actuators |
| Color | 300-nm shift in absorbance band | Displays, smart windows |
| Ion permeability | From zero to $10^{-8}$ $mol.cm^{-2}s^{-1}$ in solution | Membranes |

The development of some of these applications to commercial viability has begun for some time already. The ability to tailor the electrical properties of these systems is one of their most attractive features and, coupled with improved stability and processability relative to the original conducting polymeric systems, new applications are surely on the horizon. (Tepveera. K, 2003)[48]

- **Applications utilizing the inherent conductivity of polymer:** antistatic coating (metal and polymers), microelectronic devices; plastic chips and "stealth" material for providing a minimal radar profile for military aircraft and naval vessels. (G. Wallace 2004)[45]

- **Electrochemical switching, energy storage and conversion:** New rechargeable batteries and redox supercapacitors.

- **Polymer photovoltaics (light-induced charge separation):** photovoltaic devices.

- **Display technologies:** electrically-stimulated light emission-light emitting diodes (LED) ,and flat panel displays.

- **Electrochromics:** advertising displays, smart windows, and memory storage devices.

- **Electromechanical actuators:** artificial muscles, window wipers in space aircrafts rehabilitation gloves, electronic Braille screens and bionic ears for deaf patients.

-**Separation technologies:** novel smart-membrane and selective molecular recognition (new chromatographic separation media).

-**Cellular communication:** growth and control of biological cell cultures.

-**Controlled-release devices:** ideal hosts for the controlled release of chemical substances.

-**Corrosion protection:** new-generation corrosion protective coatings.

-**Remotely readable indicators:** electronic noses, biosensors, and biomechanic devices.

## 2.7 Polypyrrole

Polypyrrole (PPy) is a heterocycle structure, as shown in Figure 2.27. PPy was reported to be a conducting polymer by Dall'Olio *et. al.* (1968)[31]. It was prepared by oxidation in sulfuric acid as a black powder at ambient temperature. It presented with a conductivity of 8 $S.cm^{-1}$. This polymer was continually studied at IBM with the electrochemical polymerization.

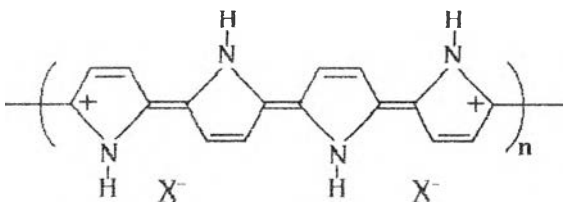


**Figure 2.27** Structure of polypyrrole.

### 2.7.1 The production of conducting polymers

The field of synthetic metals remains an active area for fundamental research in experimental and theoretical solid-state physics as well as organic and polymer synthetic chemistry. A variety of new conducting polymeric solids has been continuously discovered and area of synthesis is extremely fast moving and competitive.

Below is a summary of the major types of synthesis techniques used to prepare polypyrrole : [2],[37],[49]

1) Electrochemical polymerization,

2) Chemical polymerization,

3) Chemical vapor deposition (CVD).

#### *2.7.1.1 Synthesis of polypyrrole*

2.7.1.1.1) Electrochemical polymerization

The passage of a current through a solution results in the loss of electrons, and compounds are oxidized at the anode. Electrons are gained and compounds reduced at the cathode. This process is referred to as electrochemical polymerization when a polymer is formed. Polypyrrole is obtained by the electrochemical polymerization of pyrrole in a solvent such as acetonitile, tetrahydrofuran, propylene carbonate, methanol and so on. An electrolyte such as tetrafluoroborate or lithium perchlorate, is present, and polymerization is carried out either at constant voltage or constant current(G. Wallace 2004)[45].

The mechanism for polymerization involves the oxidation of polypyrrole at the α-position to form a radical-cation (Figure 2.28) which undergoes radical coupling to yield the dimer-dication. The latter loses two protons to yield the dimer. The dimer repeats the same reaction sequence—loss of an electron to form a dimer radical-cation, coupling with itself and to form the tetramer-dication and trimer-dication, respectively, followed by the loss of two protons to yield a tetramer. Propagation to form a polymer proceeds via repetition of the same sequence, one electron loss, coupling of different-sized radical-cations, deprotonation. This polymerization mechanism bears considerable resemblance to that for the oxidative polymerization of 2,6-disubstituted phenols (Figure 2.29).

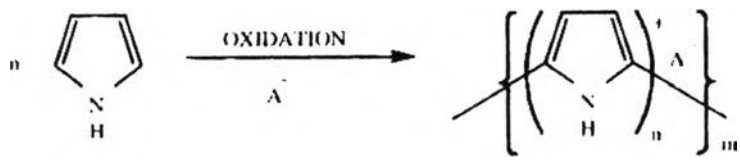


**Figure 2.28** Polymerization involved with the oxidation of polypyrrole.

**Step 1. Monomer Oxidation**

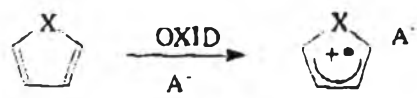


*Resonance forms:*

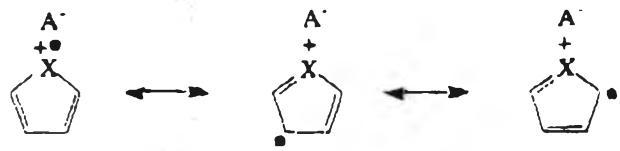


(I) (II) (III)

**Step 2. Radical-Radical Coupling**


**Step 3. Deprotonation/Re-Aromatization**

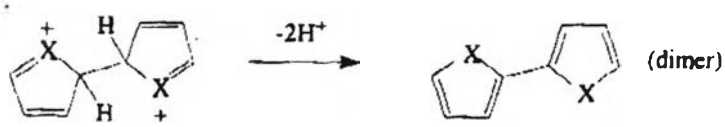


**Step 4. Chain Propagation**

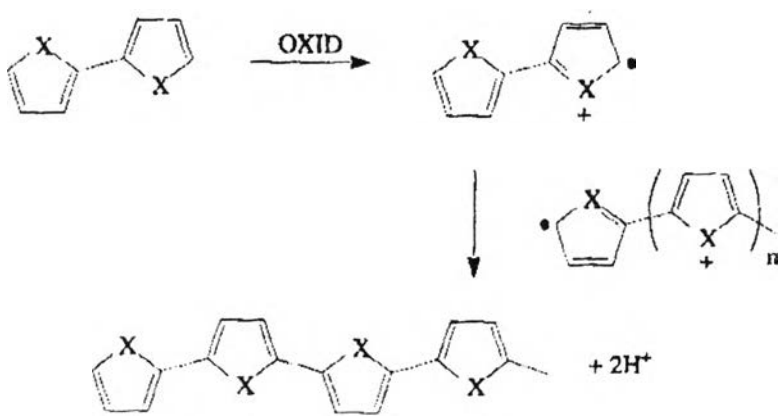


**Figure 2.29** Polymerization of polypyrrole.

Electrochemical polymerization, as usually carried out, does not yield neutral, nonconducting polypyrrole, but the oxidized (doped), conducting form. (One can cycle back and forth between the conducting and nonconducting forms, black and light yellow, respectively, by reversing polarity.)

2.7.1.1.2) Chemical polymerization in solution

The synthesis of conducting polymer via chemical method is less popular, even though this method allow a simple preparation of large quantities, and is more convenient and economical. The majority of the chemical synthesis method involves the polymerization and oxidation with oxidative transition metal ions, for example $FeCl_3$,$AgNO_3$,$Cu(NO_3)_2$, $AlCl_3$, and more. The uses of other oxidants, such as acid, halogens and organic electron acceptors, have also been reported. Considerable chemical compositions and reaction stoichiometries for polypyrrole complexes were synthesized from $FeCl_3$, based on the observed chemical compositions of the complex, particularly the [Cl] / [N] ratio. At the present time, two reaction stoichimetries have been proposed:

$$4\ C_4H_5N + 9\ FeCl_3 \rightarrow [(C_4H_5N)_4^+Cl^-] + 8\ HCl + FeCl_2$$

$$n\ C_4H_5N + 2.33n\ FeCl_3 \rightarrow [C_4H_5N{+}0.33Cl^-]_n + 2.33n\ FeCl_2{+}2n\ HCl$$

Recently, pyrrole obtained from chemical polymerization in solution can exhibit very high electrical conductivity when a suitable solvent is selected and the oxidation potential in the solution is controlled.

When in the conducting form, the electropolymerization film contains 10-35% anion (by weight) which is affiliated with the cationically–charged polymer chain. The amount of anions found in each film is governed by the level of oxidation of the polymer and is a characteristic of each film. The anion contents for the various films are listed in Table 2.7. This polymer/anion compositional balance of the films actually proves to be quite useful, since the properties of the films can be conveniently altered by changing the anion. Since the anion in the film is incorporated from the electrolyte salt in the preparative solution, the modification can be simply done by changing the electrolyte salt of the solution.

**Table 2.7** Anion content of conducting film

| Film | Oxidation level | Anion Content (%by wt) |
|---|---|---|
| Polypyrrole | 0.25-0.33 | 25-30 |
| Polythiophene | 0.06 | 7-25 |
| Polybithiophene | 0.22 | 12 |
| Azlene | 0.25 | 15-28 |
| Pyrene | 0.45 | - |
| Carbazole | 0.45 | 21 |
| Indole | 0.2-0.3 | 15-20 |
| Furan | - | 26 |

In the case of the polypyrrole films, a wide variety of anions have been used to prepare thick free standing films, seen in Table 2.8. The anions listed in Table 2.8 are poorly nucleophilic and permit the formation of good-quality films. Tetraalkylammonium salts were used in the preparation of these films. These flims are hydroscopic and will lose 5-7% moisture when dried at 110°C. The level of oxidation of polypyrrole is 0.25-0.32 per pyrrole unit, corresponding to one anion for every 3-4 units. The level of oxidation is an intrinsic characteristic of the polymer and is not sensitive to the nature of the anion. The anion, however, does influence both the structure properties and the eletroactivities of the films. The differences observed between the surfaces are not reflected in the packing structure of the bulk material. Thus, with the exception of one or two of the anions listed in Table 2.8, all of the films have similar flotation film-coating densities which are in the range of 1.45-1.51 $g/cm^3$. Polypyrrole films containing toluenesulfonate, perchlorate, and fluoroborate anions are hard and strong films and stretch very little (4-5% elongation at break).

**Table 2.8** Polypyrrole films with different anion

| Anion | Oxidation level | Density ($g/cm^3$) | $\sigma$ ($\Omega^{-1}cm^{-1}$) |
|---|---|---|---|
| Tetrafluoroborate | 0.25-0.32 | 1.48 | 30-100 |
| Hexa-fluroarsenatte | 0.25-0.32 | 1.48 | 30-100 |
| p-toluenesulfonate | 0.32 | 1.37 | 20-100 |

| | | | |
|---|---|---|---|
| Hexa-fluorophosphate | 0.25-0.32 | 1.48 | 30-100 |
| Perchlorate | 0.30 | 1.51 | 60-200 |
| Hydrogen sulfate | 0.30 | 1.58 | 0.3 |
| Fluorosulfonate | - | 1.47 | 0.01 |
| Trifluoromethyl-sulfonate | 0.31 | 1.48 | 0.3-1 |
| p-Bromo-benzenesulfonate | 0.33 | 1.58 | 50 |

**2.7. 2) Literature survey**

PPy has been mostly investigated in electrically conductive polymer. It is remarkable with high conductivity, and good stability in air and water. Additionally, it can be used in special applications such as antistatic coating, conducting paints, and electromagnetic shielding. Therefore, many methods have been proposed to prepared the composites.

Tanawadee. L.(1992)[50] prepared pure PPy which had a high electrical conductivity; the chemical polymerization of pyrrole used anhydrous ferric chloride as an oxidant. The best solvent in this method was methanol. The reaction was accomplished with 2.5 M $FeCl_3$ in methanol at 0°C for 20 minutes reaction time. Under this condition, the synthesized polypyrole showed high electrical conductivity at about 100 $Scm^{-1}$. This result introduces the new condition for the synthesis of high conductivity polypyrrole.

Ruckenstein. E. (1991)[51],[52],[53] synthesized polypyrrole composites by using a modified crosslinked porous medium, which is employed as the host for PPy deposition. Crosslinked polystyrene was prepared by the concentrated emulsion polymerization method. They prepared the composite by imbibing the host with a solution of pyrrole and subsequently with an oxidant solution. This method is an improvement of the mechanical properties by inserting the PPy particle into pores on a PS matrix. The electrical conductivity of the composite and the "penetration" of PPy in the host polymer are influenced by the polymerization conditions. However, the best conductivity value, which is about 0.8 $Scm^{-1}$, is still low.

After the PS/PPy composites were synthesized in the form of thick materials by Ruckenstein and his coworkers, processable conductive PPy/poly(alkyl methacrylate) composites were prepared by an emulsion pathway. In this method, the composite had been prepared using a two-step procedure. First, an emulsion was genereated by dispersing a chloroform solution of poly(alkyl methacrylate) and pyrrole in a small amount of an aqueous surfactant solution. The surfactants are sodium dodecyl sulfonate (SDS) and sodium dodecyl benzene sulfonate. SDS was adsorbed on the interface between the two phases, via double layer repulsion. Second, the pyrrole was polymerized and doped by stirring with an aqueous solution of ferric chloride. The polypyrrole deposited on the host polymer. The electrical conductivity could reach values as high as 1 $Scm^{-1}$, but it is still low.

Omastova, M. (1996)[54][55] studied the polypyrrole composite of PP. Like other particle composites, PPy was coated on the PP particle. $FeCl_3$ was used as the dopant of the water-methanol mixture. All compounds were stirred for a few hours. In this report, characterization by elemental analysis, infrared spectroscopy, scanning electrical microscopy (SEM) and thermogravimetric analysis was done. Additionally, the conductivity of PP/PPy composites was measured to give the range of $10^{-10}$ to$10^{-2}$ $Scm^{-1}$. This value is small compared with that of pure PPy. This report suggested the applications in antistatic packaging and electromagnetic radiation shielding.

Meng, O., Chi, M.C. (1988)[56] prepared PPy composites by the synthesis of PPy on the surface of PVC particles, which have an average size of 0.10 nm. By this method, the PVC particle was covered by PPy (Figure 2.30).

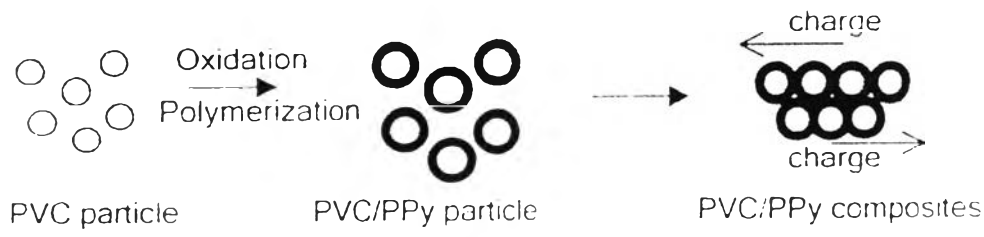


**Figure 2.30** Preparation of compressed PVC/PPy composites.

The oxidant solution is $FeCl_3$ in distilled water. The PVC/PPy products were compressed in both hot pressing and cold pressing to give samples that were measured by the conductivity measurement. The PVC/PPy composite samples have a continuous surface after compression. This raises the conductivity along the surface materials. The optimum electrical conductivity is ~$10^{-1}$ $Scm^{-1}$.

Lascelles. S.F.. and Armes. S.P. (1997)[57],[58] synthesized near-monodispersed micrometresize, polypyrrole-coated PS latexs with various conducting polymer loadings. PPy was polymerized to cover PS particles, which have an average size of 1.6 μm. They show the schematic representation of an isolated, micrometer-sized, polypyrrole-coated PS particle (Figure 2.31).

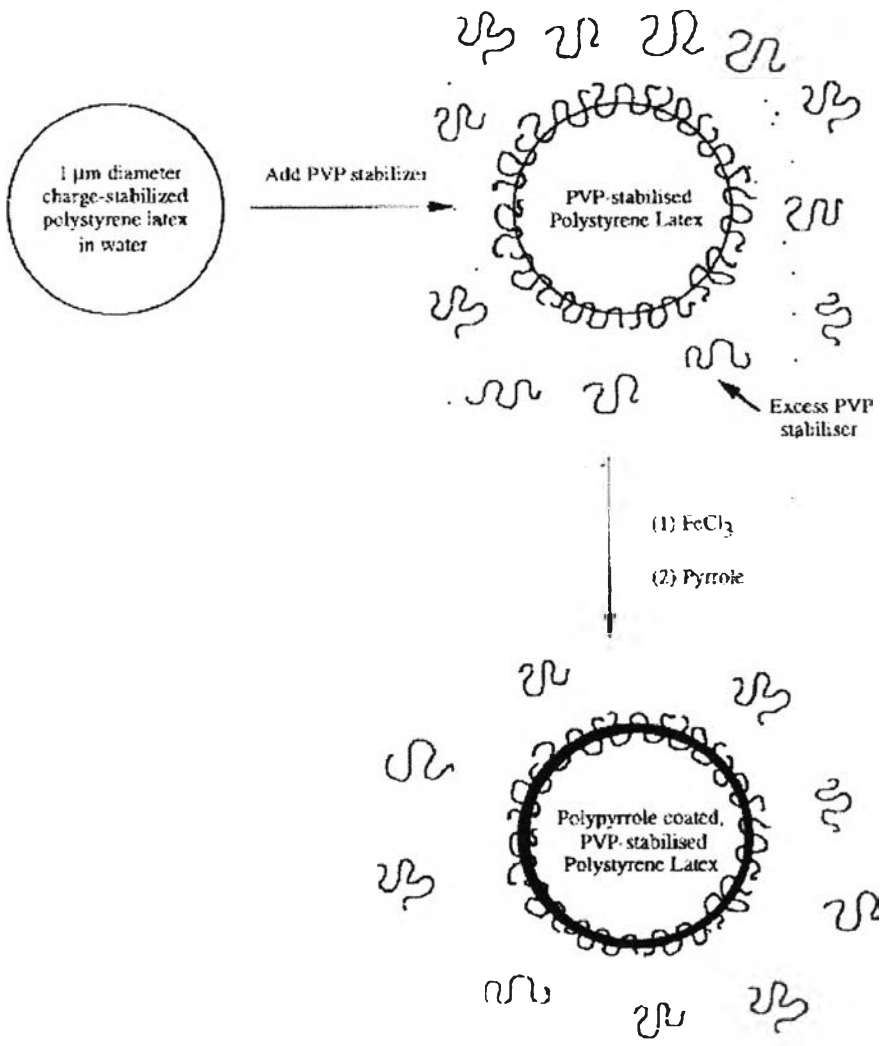


**Figure 2.31** Polypyrrole-coated PS particle using PVP as stabilizer

Lascelles and Armes (1997) also synthesized Poly(N-vinylpyrrolidone) and used as stabilizer, which they suggest that the conducting polymer be formed as a thin layer at surface of the latex particles. This is the "Core-shell" morphology (Figure 2.32), which was made by dissolving PVP in an aqueous dispersion of PS latex. The conductivity of this composite is about 1 $Scm^{-1}$, which is higher than other PPy particle composites. Further, the IR spectra of dried polystyrene latex and polypyrrole-coated polystyrene were shown. The spectra reveal an enhanced adsorption effect with a change of the coating polypyrrole percentage. Potential applications for these micrometer-sized coated latexes including an improved stationary phase for electrochromatography and "novel marker" particles for visual agglutination diagnostic assays.

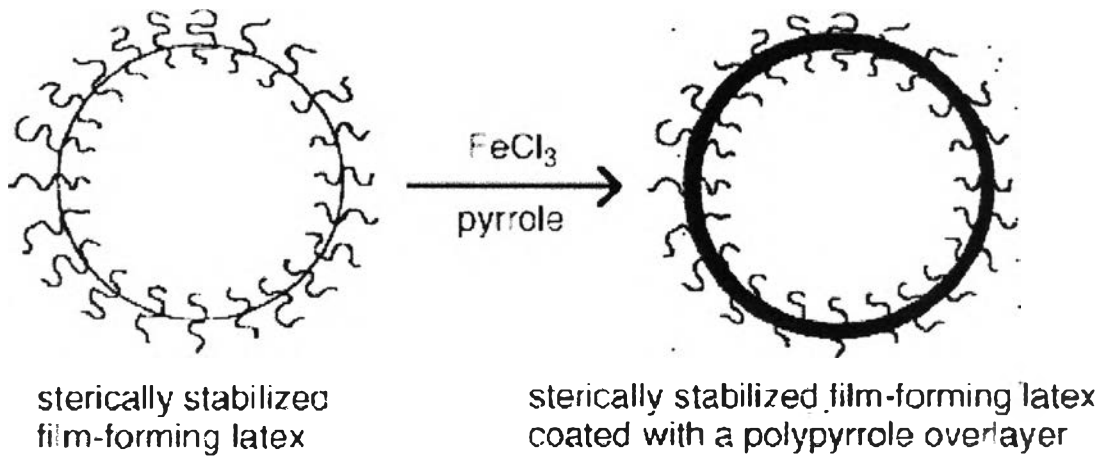


**Figure 2.32** Schematic formations of polypyrrole-coated latex particles as core-shell structure.

Moreover, for the dispersion polymerization method (Armes, S.P. and Vincent. B., 1987), many reaction systems were investigated. Armes and Vincent prepared the conducting PPy particles in dispersion polymerization containing dispersing agents, PVA, PVP, and various cellulose derivatives were used to stabilize the shape of the polypyrrole particles. They suggested that using an aqueous media of $FeCl_3$ as the initiator could produce high electrical conductivity to polypyrrole particles. The colloidal polyprrole particle was the result of stabilizing the system in aqueous media, which comprised of ethanol, water, and any dispersing agent.

Copper. C.E. and Vincent. B. (1989)[59] also proposed the preparation of electrically conductive films by casting aqueous dispersion of mixed polymer lattices on supporting glass microscope slides. The mixed polymers are the composition of conducting polymer(polypyrrole or polyaniline) and other film forming, a 1:1 copolymer of polymethyl methacrylate and polybutylacrylate. Conducting polypyrrole was prepared as the dispersion particle form by using poly(vinyl alcohol-co-vinyl acetate) as the dispersing agent. As in the other report, the maximum conductivity is too low, i.e. about 0.1-2 $Scm^{-1}$.

Tieke et al. (1990)[60] studied electrical conductivity with high thermal stability up to 350 °C in polypyrrole/ polyimide composite films, which were prepared either by the electrochemical polymerization of pyrrole on a polyimide-coated electrode or by exposing polyimide films containing $FeCl_3$ as oxidant to pyrrole vapor. Films prepared by the electrochemical route consist of a sequence of three layers with polyimide sandwiched between the layers of pyrrole. These films show a maximum conductivity of about 10 S/cm. The chemically manufactured films consist of polyimide containing finely dispersed polypyrrole particles of 10 to 500 nm. in diameter with a maximum conductivity of $5x10^{-4}$ $S.cm^{-1}$. However, previous research was limited by the diffusing of the oxidant inside the film. This obstacle could be partly avoided by using insulating films, in which the ionic dopant is already bound to the polymer backbone, via ionomers.

Digar et al. (1994)[61] prepared dispersion PPy at room temperature by oxidative polymerization using an $FeCl_3$ oxidant in the presence of poly(vinyl methyl ether) (PVME) as the stabilizer and ethanol or aqueous ethanol as the dispersant. They proposed that, with water as the dispersion medium, lower temperatures are required when a solvent property of water towards the PVME stabilizer becomes good enough to affect steric stabilization. PPy prepared in 50% ethanol or in water exihibit specific conductivity, about 10 $Scm^{-1}$.

Zoppi et al.(1997)[62] studied the semi-interpenetrating network of polypyrrole and ethylene-propylene-5-ethylidene-2 –norrbornene rubber, EDPM, were prepare by the chemical oxidation of a monomer using two different method of synthesis. In the first method, EPDM rubber samples containing $CuCl_2$ and dicumyl peroxide were obtained by mechanical mixing, crosslinked by heating, and exposed to pyrrole va-

pors. In the second route, EDPM rubber crosslinked with dicumyl peroxide was swollen in an $FeCl_3$/THF solution and exposed to pyrrole vapors. Both methods provide semi-IPN of polypyrrole/EDPM rubber, but the electrical conductivities of the materials obtained by the second route ($\sigma=10^{-5}$ S/cm$^{-1}$) are higher than by the first route ($\sigma=10^{-10}$ S/cm$^{-1}$). However, thermal aging showed that the electrical conductivity decreases as a function of the heating time.

Lauhasurayothin, S. (1999)[63] prepared polypyrrole (PPy) composites. PPy was synthesized by chemical oxidation method in the presence of PS particle using $FeCl_3$ as the oxidant. PPy was covered on PS and analyzed by attenuated total reflectance spectroscopy. Other host polymers were attempted, including polyvinyl chloride (PVC), polyethylene (PE), and polypropylene (PP). The results indicated that the PPy/PS composites and PPy/PVC composites have a conductivity as high as 10 S/cm.

J.vilcakova (2004)[65] studied the electrical conductivity of a silicone rubber/ polypyrrole composite in the presence of ferric chloride as an oxidant and DBSNa as anionic surfactant by using chemical polymerization as a technique. The polyprrole percolation threshold concentration in silicone rubber/ polyprrole composites was found to be low 4 vol%. The sample containing polypyrrole above the percolation threshold showed only a slight conductivity increase when the compression was lower than 8%. At a compression deformation higher than 11%, a significant steep decrease in conductivity, more that five orders of magnitude (Figure 2.33), together with a good reproducibility analogous to switching off the electrical contacts were observed. He also studied the morphology of a PPy-Cl-DBSNa sample by SEM at higher magnification revealing the presence of globular particles (Figure2.34). The results showed that the particles formed irregular aggregates, which may be caused by the imperfect contacts of PPy particles creating a continuous conducting network. As in other reports, the maximum conductivity was too low.

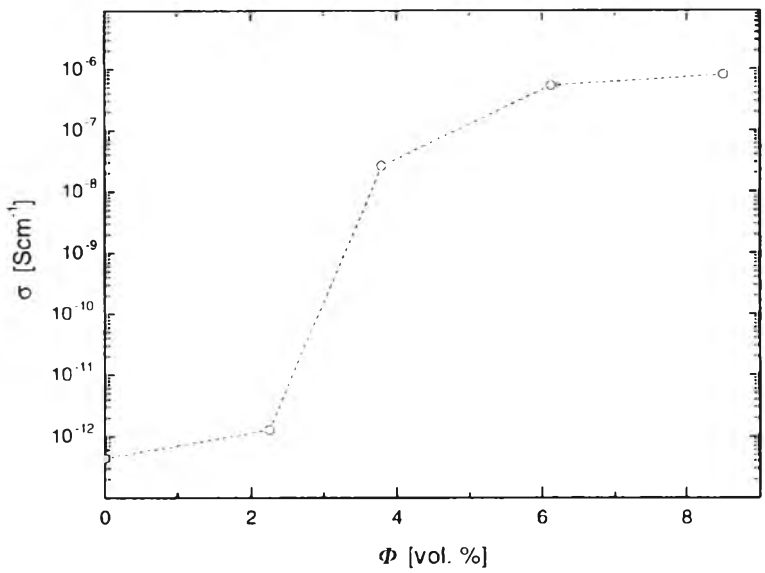


**Figure 2.33** Dependence of electrical conductivity on the PPy concentration.

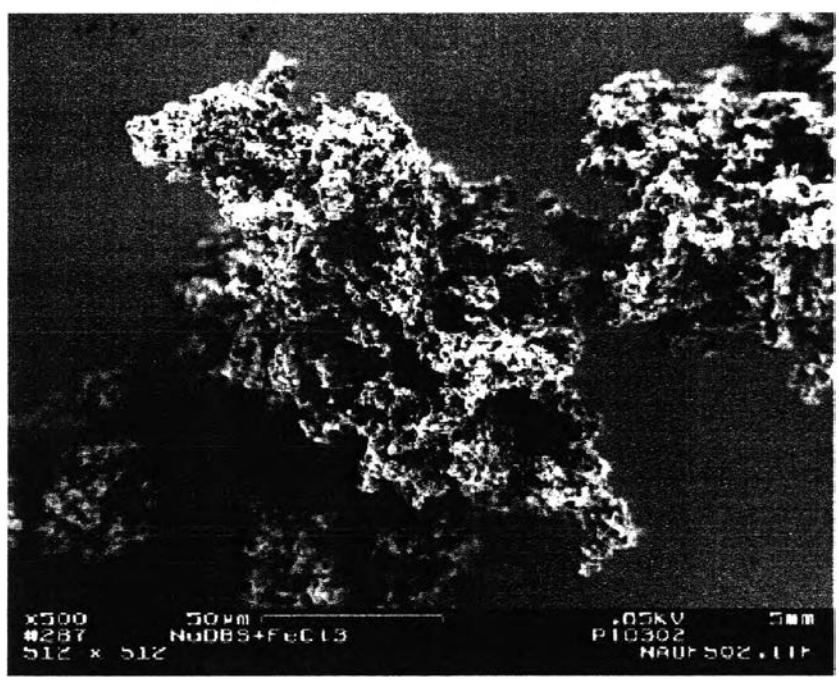


**Figure 2.34** Scanning electron micrograph of polypyrrole.

However, there are several limits for conventional use as a conducting polymer. It suffers from poor mechanical properties, e.g. brittleness, low processibility, and is hardly obtained with a controlled conductivity.

Anuar et al. (2006)[66] studied the electrochemical preparation of polypyrrole-polyethylene glycol (PPy-PEG) conducting polymer composite films on an indium tin oxide glass electrode from an aqueous solution containing pyrrole monomer, p-toluene sulfonate(p-TS) dopant, and polyethylene glycol(PEG) insulating polymer. They found that (PPy-PEG) conducting polymer composite films with very good conductivity can be prepared electrochemically. The electrical conductivity of the composite film is influenced by the concentration of the dopant.

Admicellar and electrochemical polymerization of PPy coated on NR latex particles was carried out in this study in order to produce ultra thin PPy film on latex particles. The mechanical strength and processibility of PPy will be examined.

## 2.8 Polythiophene

Polythiophene has much in common with polypyrorole. Thiophene is oxidized to form a conducting electroactive polymer with the greatest conductivity obtained from the α-α linkages. Thiophene was found in tar, gas, and industrial benzene obtained from coal. Polythiophene and its derivatives is largely motivated by their multiple potential technological applications. These applications can be divided into three main groups resorted to (G. Wallace 2004)[45]:

- The electrical properties of the doped conducting state, such as antistatics and EMI shielding, PT-based gas sensors, PT-based radiation detectors and corrosion protective films.
- The electronic properties of the neutral semiconducting state, such as photovoltaic cells and nonlinear optics.
- The electrochemical reversibility of the transition between the doped and the undoped state such as in new rechargeable batteries, display devices, electrochemical sensors, and modified electrodes (Tepveera. K. 2003)[48].

The polymerization of thiophene was first reported in the last century. However, only in the last two decades was extensive research carried out regarding polythiophene and its derivatives. The thiophene units in polythiophene are linked through both the 2- and 3- positions; the irregularity caused by the units involving the 3-position decreases the conductivity of polythiophene because it interrupts the long delocalized π -bond of those linked through the 2-position. However, when the 3-position of the thiophene unit is occupied by an organic group, such as in the 3-alkylthiophene, the conductivity of the polymer increases in a major way, because of increased linkage ordering.

Since polythiophene is insoluble, infusible, and brittle, and hence unprocessable, methods were developed to increase its processability and properties. Admicellar and electrochemical polymerization of PTh coated on NR latex particles was carried out in this study similar to the PPy method.

2.8.1 Synthesis of Thiophene[45],[48]

Polythiophene(Figure 2.35) can be synthesized either electrochemically or chemically using simple oxidation.

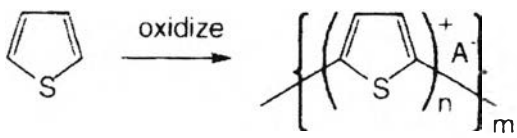


1

**Figure 2.35** Polymerization involve with oxidation of Thiophene.

*2.8.1.1) Electrochemical polymerization*

As with PTh, n is usually between 2 and 4; $A^-$ is a counterion incorporated into the polymer during growth to balance the charge on the polymer backbone; and m is a parameter proportional to the molecular weight.

The mechanism of polymerization involves the formation of radical cations (Figure 2.36) that react with each other or with starting monomers to develop the polymeric structure.

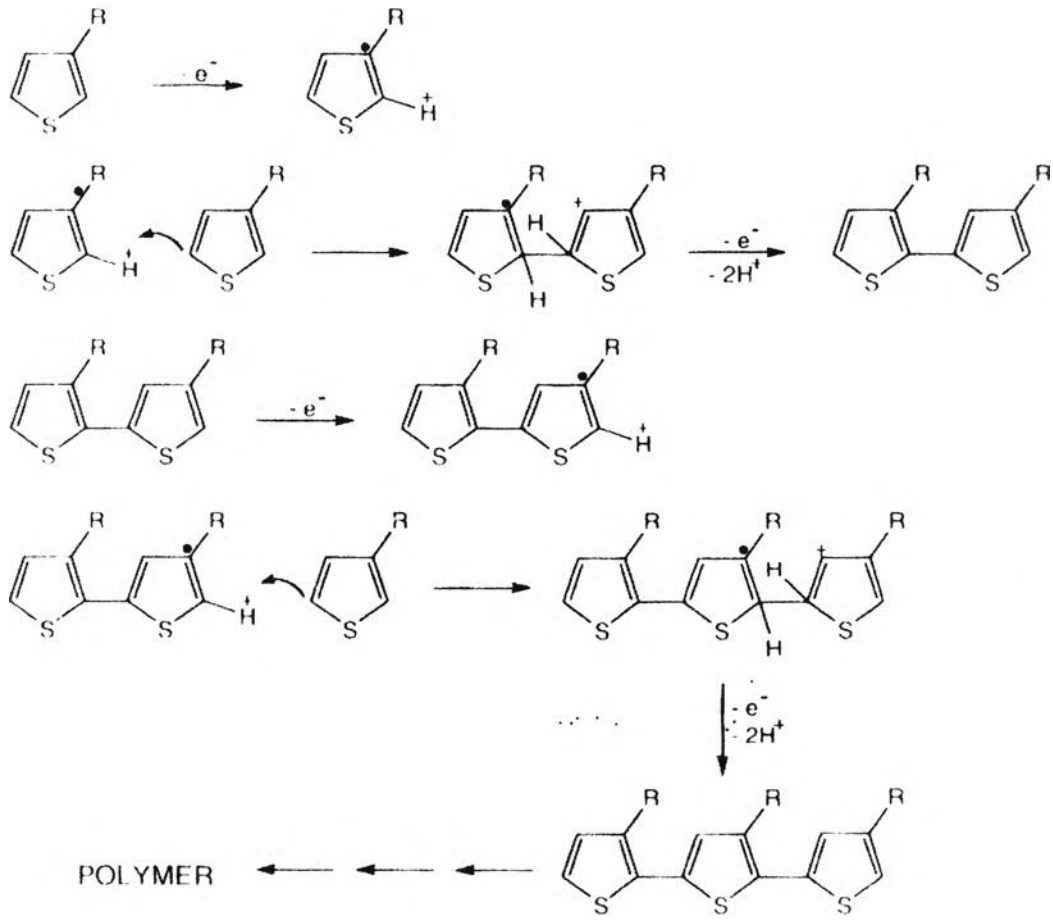


**Figure 2.36** Polymerization of thiophene.

**Substituted polythiophene**

Among the various possible strategies for the modification of a conducting polymer, the polymerization of monomers modified by the covalent grafting of functional groups represents the most straightforward method to achieve control at the molecular level of the structures, electronic and electrochemical properties of conducting polymer. Consequently, the synthesis of a conducting polymer from a substituted monomer in respect to the above prerequisites implies a detailed comprehension of the structural effects of substitution (inductive, mesomeric, and steric) at various stages of organization of the material.

**Polythiophene(3-substituted thiophene)**

The introduction of long chain alkyl groups at the 3-position of thiophene unit in polythiophene converts the polythiophene into a class of identifiable, soluble and processable conducting polymers. The design and synthesis of specially structured poly(3-subsituted thiophenes) have become an area of active interest. The variation of 3-substituents on the thiophene rings has a pronounced effect on the physical properties of the polythiophenes

Elsenbaumer et al. (1985)[66] reported the first synthesis of soluble poly(3-alkylthiophene) in 1985, permitting the casting of thin films of the polymers. The nonsymmetrical 3-alkylthiophene monomer unit gives four possible neighboring environments for a given unit in the polymer. Usually these four enchainments are indicated as HT-HT (Head-to-Tail, Head to Tail) for the regioregular enchainment, TT-HT, HT-HH, and TT-HH (Figure 2.37).

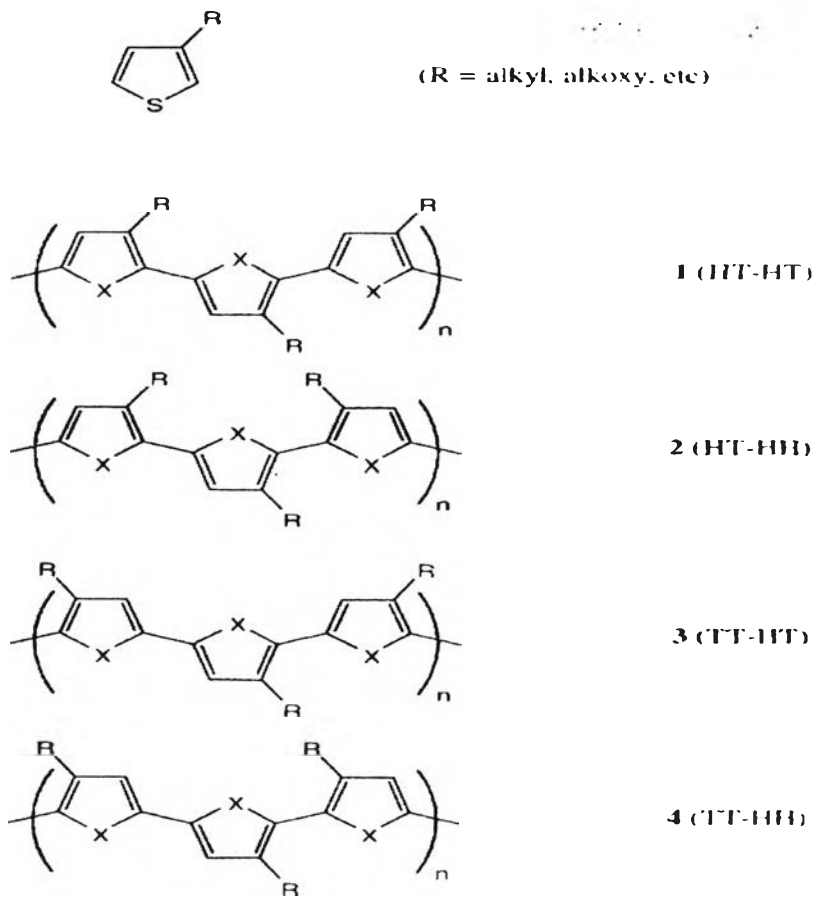


**Figure 2.37** Structure of polythiophene.

In the quest for a soluble and processable conducting polythiophene, alkylthiophenes were polymerized. Since 3-alkylthiophene is not a symmetrical molecule, there are three relative orientations available when two thiophene rings are coupled between the 2- and 5-positions. The first of these is 2-5' or head-to-tail coupling (HT), the second is 2-2' or head-to-head coupling (HH), and the third is 5-5' or tail-to-tail coupling (TT) (Figure 2.38). [68-78]

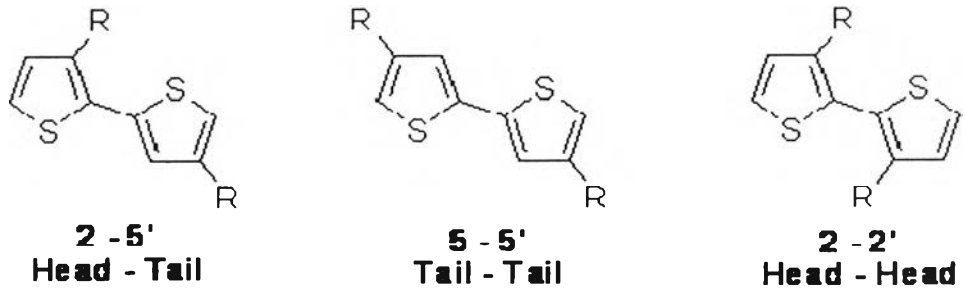


**Figure 2.38** Possible reiochemical coupling of 3-alkylthiophene[68-78]

The relative occurrence of these regioisomeric variations in the enchainment depends on the polymerization method. Grignard Synthesis[67-78] usually gives the highest amount of regioregular polymer (70-98%), electrochemical polymerization gives the least (50-60%) while chemical polymerization with $FeCl_3$ as a catalyst occupies a middle position (50-70%) (Tepveera. K. 2003)[48]. From the UV-visible spectrum, high regularity poly(3-alkylthiophene) (93-98% HH-HT couplings) shows bathochromic absorption in comparison to regiorandom poly(3-alkylthiophene) that was prepared by oxidative polymerization with $FeCl_3$. These data are indicative of longer effective conjugation lengths of regioregular head to tail poly(3-alkylthiophene). The effect of this microstructural irregularity is to create a sterically driven twist of the thiophene rings out of coplanarity and conjugation with one another. This is illustrated by the structure diagram in Figure 2.39. [68-78]

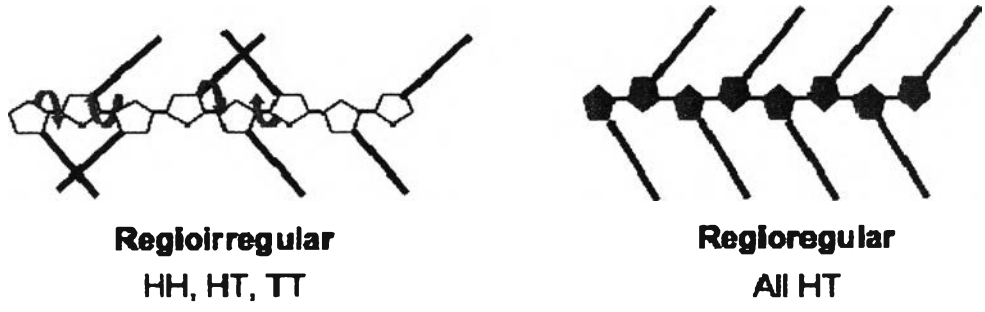


**Figure 2.39** Regioirregular vs. regioregular poly(3-substituedthiophene).[68-78]

*2.8.1.2) Chemical polymerization*

The method is easily accessible to almost all scientists who wish to obtain poly(3-alylthiophene) and will provide a sufficient amount of the polymer for general use. The oxidative coupling reaction of 3-alkylthiophene by $FeCl_3$ are shown in Figure 2.40.

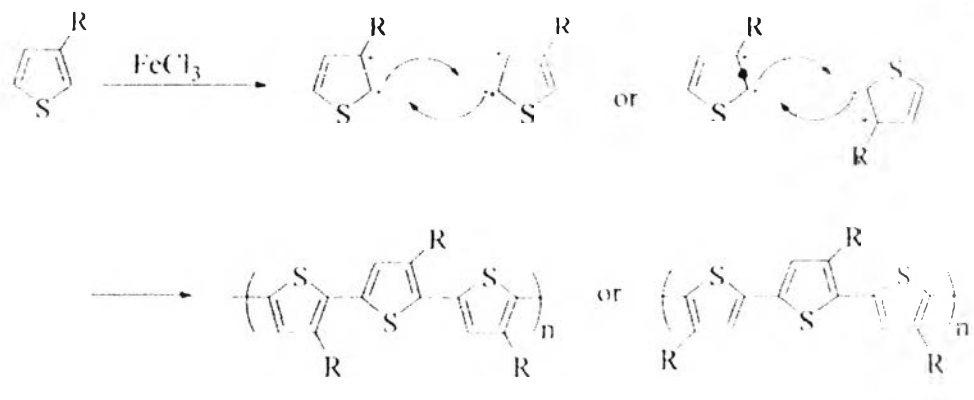


**Figure 2.40** Oxidative coupling reaction of 3-alkylthiophene by $FeCl_3$.

The general observation of increased stiffness and strength for the reduced polythiophene is the opposite of that observed for polypyrrole. In PPy, the oxidized state was observed to be stiffer and stronger, but less ductile than the reduced state due to the ionic crosslinking that is induced by the ionic nature of the polymer. In the case of polythiophene, it is possible that the increase in solvent content that accompanies oxidation causes a plasticization effect that is greater than the ionic crosslinking, so that the oxidized flim is more ductile and flexible.

### 2.8.2 Literature Survey

Masuda et al (1999)[79] considered the morphology of PThs produced by an entirely different electrochemical procedure. It was shown that the determinants of PThs morphology are more complex as with other conducting polymers. However, the effects on mechanical and electrical properties, as well as switching properties, are likely to be significant and worthy of further investigation. To achieve high conductivities, the polythiophene paradox must be overcome and using the galvanostatic polymerization method. Synthesis at reduced temperatures will help to avoid overoxidation and increase the conductivity of the resultant material. Conductivity as high as 7,500 S $cm^{-1}$ has been obtained for poly(methylthiophene).

Most interest has focused on problems due to improved mechanical properties by using the electrochemically to prepared films. Ito and co-workers (1996)[139] observed that the mechanical properties (E, $\sigma_b$ , and strain at break, $\varepsilon_b$ ) of electrochemically reduced PTh films were all increased compared as with the prepared oxidized films.

Yigit et al.(1996)[81] determined the thermal behaviors and degradation products of conducting polymer composites prepared by the electrooxidation of thiophene using natural rubber or synthetic rubber as the insulating matrix. The pyrolysis mass data revealed that the chemical interaction formed between the components of the composites during polymerization. Thermal characteristics of rubbers totally disappeared in the composites, indicating the presence of some chain scission leading to degradation of the rubber during electrooxidative polymerization.

Melike et al. (1999)[82] investigated the electrochemical properties of thiophene and polythiophene(PTh) in tetrabutyl ammoniumperchlorate, tetraethyl ammoniumtetrafluoroborate and tetrabutyl ammoniumhexafluorophosphate supporting in electrolytes in acetonitrile. Polarization curves and in situ conductance measurements showed that PT film had different electrochemical properties and conductance values according to the type and concentration of the supporting electrolyte employed.

Louzhen(2005)[83] synthesized a hybrid thin film of endohedral metallofullerene ($Dy@C_{82}$) and polythiophene by using the electrochemical method Figure 2.41. The data suggest that the $Dy@C_{82}$ molecules have been uniformly dispersed in the polythiophene matrix, forming a compact film.

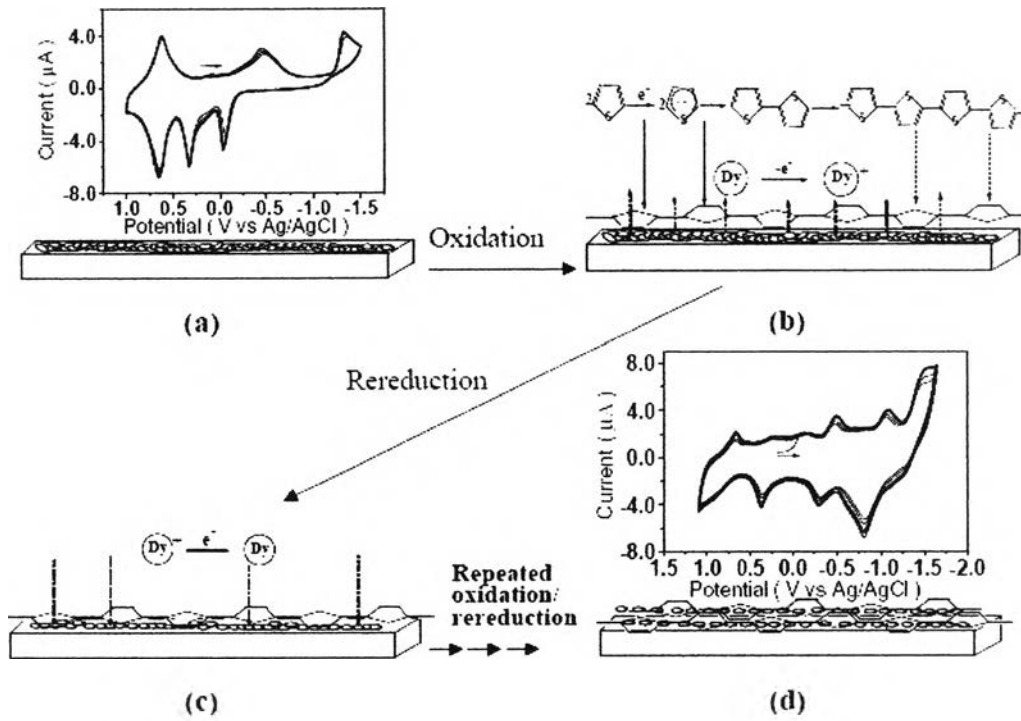


**Figure 2.41** A schematic showing the mechanism for the hybridization of Dy@C82 and PT via electro-polymerization and redox-enhanced mixing.

Semih et al. (1996) [84],[85] synthesized the electrochemical of conducting polymer composites of polythiophene.The electrooxidation of thiophene (Th) using an SR- and NR-coated on a Pt anode are black film which can be peeled of from the Pt electrode surface. During electrolysis, the PTh film turns from green to black as the doping state increases. The conductivity measurement was done by using a standard four point probe technique. The measured conductivities according to the weight percentage of the PTh in composite blends (with natural rubber (NR) and synthetic rubber (SR)) are given in Table2.9. The high percentage of thiophene in the composites is due to losses in rubber content during PTh polymerization. This did not allow us to obtain high rubber content composite films.

**Table 2.9** Conductivity of composite films [84].[85]

| %PTh | Conductivity of SR-PTh | Conductivity of NR-PTh |
|---|---|---|
| 65 | $1 \times 10^{-1}$ | -N/a- |
| 75 | $2 \times 10^{-1}$ | -N/a- |
| 80 | $2.6 \times 10^{-1}$ | $3 \times 10^{-1}$ |
| 85 | $3 \times 10^{-1}$ | $3.5 \times 10^{-1}$ |
| 90 | $4 \times 10^{-1}$ | $3.2 \times 10^{-1}$ |
| 95 | $6 \times 10^{-1}$ | $3.7 \times 10^{-1}$ |

Yasemin et al. (2005)[86] synthesized a soluble sulfonated conductive co-polymer by electrochemical oxidation in anhydrous $FSO_3H$. The sulphur-to-nitrogen ratios indicated that copolymers were formed in addition to the incorporation of $SO^-_3$ group into the polymeric backbone. The sulfonated copolymer films have better solubility in DMSO and KOH. As a result, the conductivity of the copolymer films increase with the increase in the number of thiophene rings in the polymeric blackbone (Table 2.10).

**Table 2.10**

The degree of sulfonation ratios (S/N ratios) and dry conductivity values of the polymer films obtained from the acetonitrile/0.1M $LiBF_4$ solutions containing 300mM aniline, 75mM $HSO_3F$, and different concentrations of thiophene

| Polymer | S/N (freshly prepared film) | S/N (reduced film) | Conductivity ($Scm^{-1}$) (freshly prepared film) |
|---|---|---|---|
| 300mM An | – | – | 0.058 |
| 300mM An + 75mM $HSO_3F$ | 0.37 | 0.10 | 1.0 |
| 300mM An + 75mM $HSO_3F$ + 150mM Ty | 4.5 | 3.8 | 1.2 |
| 300mM An + 75mM $HSO_3F$ + 200mM Ty | 5.5 | 5.3 | 1.8 |
| 300mM An + 75mM $HSO_3F$ + 300mM Ty | 8.3 | 6.7 | 2.4 |
| 300mM An + 75mM $HSO_3F$ + 400mM Ty | 10 | 11 | 4.8 |
| 300mM An + 75mM $HSO_3F$ + 500mM Ty | 11 | 12 | 5.7 |
| 400mM Ty + 75mM $HSO_3F$ | – | – | 6.2 |
| 200mM Ty | – | – | 21 |

Xi-Shu Wang et al. (2002)[87] synthesized the polythiophene thin film in a one compartment cell with the use of an EG&G potentiostat, model 283, under computer control. The mechanical properties of conducting polythiophene (Pth) films were investigated with SEM to understand the relation between the mechanical properties and the electrochemical polymerization deposition process and microstructure, as well as film thickness. The fatigue microcrack initiation and growth around a cross indent was observed in low cycle tension-tension fatigue tests (Figure 2.42).

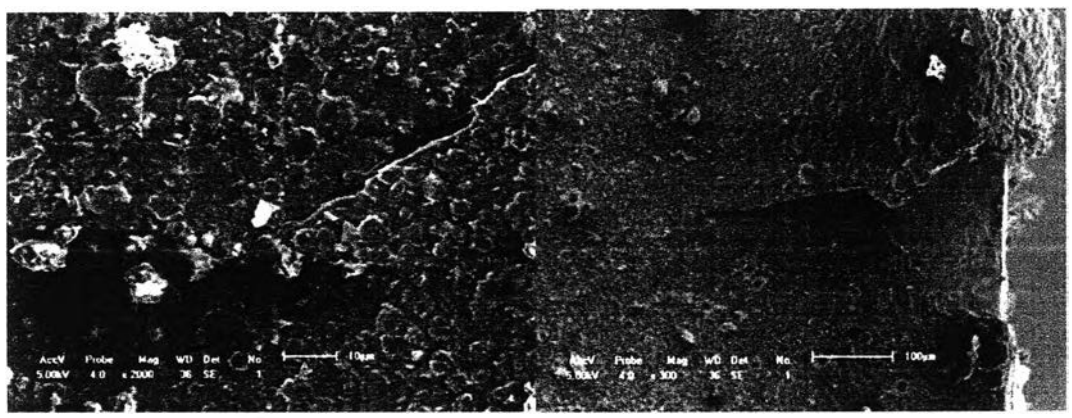

**Figure 2.42** Fatigue fracture types of a conducting Pth coating film on a substrate. (Left) A spalling fracture type caused by fatigue loading. (Right) A fragmentation fracture type caused by fatigue loading.

Yue. S. (1995)[88] studied the inverted emulsion pathway and employed it to prepare poly(3-methylthiophene) rubber conductive composites. In the first step, an inverted emulsion containing an aqueous solution of $FeCl_3$ as the continuous phase was generated. In the second step, a toluene solution of 3-methylthiophene was introduced dropwise into the inverted emulsion where the monomer was polymerized by the oxidant $FeCl_3$ to the conductive polymer. After the completion of polymerization, the composite was obtained by precipitating the conductive polymer and the host polymer. Under suitable preparation conditions, composites with both high conductivities and good mechanical properties were obtained; these composites had a conductivity as high as 1.3 S/cm as well as a tensile strength of 14.8 MPa and an elongation of 84% at break point. Among thiophene, 2,2'- bithiophene and 3-methylthiophene, the latter monomer was the most suitable for preparing the thiophene-containing conductive composite by the inverted emulsion method.